

# Accepted Manuscript

Microwave-assisted one-pot synthesis of new phenanthrene fused-tetrahydrodibenzo-acridinones as potential cytotoxic and apoptosis inducing agents

Niggula Praveen Kumar, Pankaj Sharma, T. Srinivasa Reddy, Nagula Shankaraiah, Suresh K. Bhargava, Ahmed Kamal



PII: S0223-5234(18)30312-X

DOI: [10.1016/j.ejmech.2018.03.069](https://doi.org/10.1016/j.ejmech.2018.03.069)

Reference: EJMECH 10334

To appear in: *European Journal of Medicinal Chemistry*

Received Date: 29 January 2018

Revised Date: 21 March 2018

Accepted Date: 22 March 2018

Please cite this article as: N.P. Kumar, P. Sharma, T.S. Reddy, N. Shankaraiah, S.K. Bhargava, A. Kamal, Microwave-assisted one-pot synthesis of new phenanthrene fused-tetrahydrodibenzo-acridinones as potential cytotoxic and apoptosis inducing agents, *European Journal of Medicinal Chemistry* (2018), doi: 10.1016/j.ejmech.2018.03.069.

This is a PDF file of an unedited manuscript that has been accepted for publication. As a service to our customers we are providing this early version of the manuscript. The manuscript will undergo copyediting, typesetting, and review of the resulting proof before it is published in its final form. Please note that during the production process errors may be discovered which could affect the content, and all legal disclaimers that apply to the journal pertain.

## Graphical abstract

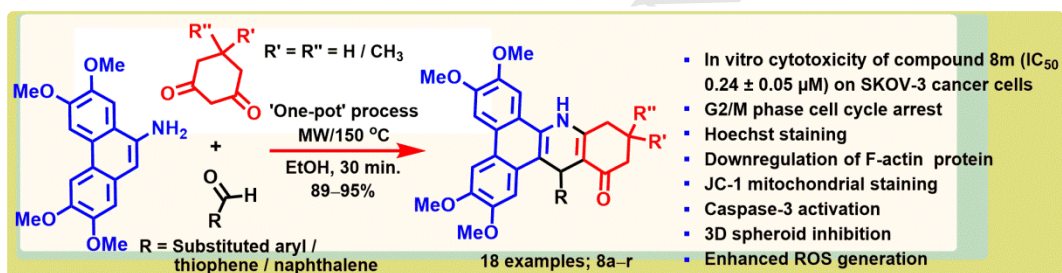
### Microwave-assisted one-pot synthesis of new phenanthrene fused-tetrahydrodibenzo-acridinones as potential cytotoxic and apoptosis inducing agents

Niggula Praveen Kumar,<sup>a</sup> Pankaj Sharma,<sup>a</sup> T. Srinivasa Reddy,<sup>c\*</sup> Nagula Shankaraiah,<sup>a\*</sup> Suresh K. Bhargava,<sup>c</sup> Ahmed Kamal<sup>a,b\*</sup>

<sup>a</sup>Department of Medicinal Chemistry, National Institute of Pharmaceutical Education and Research (NIPER), Hyderabad 500 037, India

<sup>b</sup>School of Pharmaceutical Education and Research, Jamia Hamdard University, New Delhi 110062, India

<sup>c</sup>Centre for Advanced Materials & Industrial Chemistry (CAMIC), School of Science, RMIT University, GPO BOX 2476, Melbourne-3001, Australia



## Microwave-assisted one-pot synthesis of new phenanthrene fused-tetrahydrobenzo-acridinones as potential cytotoxic and apoptosis inducing agents

Niggula Praveen Kumar,<sup>a</sup> Pankaj Sharma,<sup>a</sup> T. Srinivasa Reddy,<sup>c\*</sup> Nagula Shankaraiah,<sup>a\*</sup> Suresh K. Bhargava,<sup>c</sup> Ahmed Kamal<sup>a,b\*</sup>

<sup>a</sup>*Department of Medicinal Chemistry, National Institute of Pharmaceutical Education and Research (NIPER), Hyderabad 500 037, India*

<sup>b</sup>*School of Pharmaceutical Education and Research, Jamia Hamdard University, New Delhi 110062, India*

<sup>c</sup>*Centre for Advanced Materials & Industrial Chemistry (CAMIC), School of Science, RMIT University, GPO BOX 2476, Melbourne-3001, Australia*

**Abstract:** An expeditious microwave-assisted one-pot synthesis of new cytotoxic phenanthrene fused-tetrahydrobenzo-acridinones has been successfully accomplished. This protocol offers wide substrate scope, catalyst-free synthesis, atom-economy, simple recrystallization, high yields, and ethanol was used as green solvent. These new compounds were tested for their *in vitro* cytotoxicity against cervical (HeLa), prostate (PC-3), fibrosarcoma (HT-1080), ovarian (SKOV-3) cancer cells, and were safer to normal (Hek-293T) kidney cell line. All the compounds have displayed significant cytotoxicity profile, among them **8m** being the most potent compound with an IC<sub>50</sub> 0.24 ± 0.05 μM against SKOV-3 ovarian cancer cells. Flow cytometry analysis revealed that cells were blocked at the G2/M phase of the cell cycle. The effect of **8m** on F-actin polymerisation was also studied. Hoechst staining clearly showed the decreased number of viable cells and indicated apoptosis progression. Compound **8m** caused the collapse of mitochondrial membrane potential as observed via JC-1 staining and also enhanced the generation of reactive oxygen species. The increase of caspase-3 activation by 3.7 folds supported the strong apoptosis induction. In addition, an *in vitro* 3D-spheroid progression assay was performed with **8m** that significantly suppressed the tumour cells.

**Keywords:** Microwave reaction, Perkin-condensation, phenanthrene fused-tetrahydrobenzo-acridinones, cytotoxicity, 3D-spheroid inhibition, apoptosis.

\*Corresponding authors: Dr Ahmed Kamal, E-mail: [ahmedkamal@iict.res.in](mailto:ahmedkamal@iict.res.in); Dr Nagula Shankaraiah, E-mail: [shankar@niperhyd.ac.in](mailto:shankar@niperhyd.ac.in); [shankarnbs@gmail.com](mailto:shankarnbs@gmail.com); T. Srinivasa Reddy, E-mail: [srinivasareddy.telukutla@rmit.edu.au](mailto:srinivasareddy.telukutla@rmit.edu.au).

## 1.0 Introduction

Cancer has been regarded as a life threatening disease to the mankind and the number of cases has been enormously increasing in the developed countries [1]. Chemotherapy is the effective treatment to combat cancer [2]. Cytotoxic agents that can induce apoptosis have an invaluable role in cancer chemotherapy [3]. Most of the cytotoxic agents are either natural origin or natural product derivatives [4]. Natural products such as phenanthrene alkaloids mainly isolated from the plant species belonging to *Asclepidaceae* and *Moraceae* family. Due to their diverse pharmacological profile they became the targets for their structural modification [5]. They have been reported to possess anticancer [6], anti-microbial [7], anti-inflammatory [8], anti-lupus [9] and anti-angiogenic [10] properties. These nitrogen-containing alkaloids are not only recognised for their potent antiproliferative activity but also significantly inhibit cancer cells resistant or cross resistant to most of the clinical drugs [11]. Phenanthrene alkaloids can induce cell apoptosis and inhibits the enzymes which involved in cell division [12]. The structurally identical molecules are not functional mimics and elicit action through binding to multiple targets [13]. These alkaloids contain a common pentacyclic skeleton similar to phenanthrene ring fused with either six-membered quinolizidine E ring or a five-membered indolizidine E ring [14]. Previous SAR studies suggest that quinolizidine derivatives are highly potent when compared to indolizidine containing phenanthrene derivatives [15]. Moreover, tylophorine, antofine and cryptopleurine are some of the representative alkaloids having broad spectrum of activity from this class [16].

Similarly, podophyllotoxin is the natural tetralin lignan mainly present in the plants of *Podophyllum emodi* and *P. peltatum* [17]. Efforts made to use podophyllotoxin as clinical drug candidate were unsuccessful due to various side effects such as nausea and damage to normal tissues [18]. However, its role as a lead in anticancer drug research has promoted the development of potent chemotherapeutic agents like etoposide and teniposide which are currently used for the treatment of various malignancies such as lymphoma, small cell lung cancer, kaposi sarcoma and testicular carcinoma [19]. Due to their structural complexity in the creation of four stereo centres at C ring, it is difficult task to prepare their analogues from easily available raw materials [20]. However, the stereo chemical complexity can be minimized by elimination of C-2 and C-3 stereogenic carbons [21]. In this context, a number of medicinal chemists made considerable efforts towards the development of 4-aza

podophyllotoxin (**7**) and its derivatives (**Figure 1**) to retain the similar cytotoxicity to that of podophyllotoxin [22].

Next, microwave-assisted syntheses of bioactive scaffolds have gained prominent status in the present medicinal chemistry research [23]. These reactions minimize the reaction time, facilitate the reaction to proceed fast in a specific manner [24] and significantly reduce the rate of decomposition of the final product when compared to conventional heating. Similarly, one-pot protocols enable the chemists to access diverse array of bioactive molecules with wide substrate scope by minimizing the synthetic steps, greater atom-economy and eliminate the tedious work-up procedure. In addition, the reactions need to be performed by using environmentally benign solvents from the green chemistry point of view [25]. Moreover, exploring synthetic precursors to gain fast access to the diversified library of new scaffolds is the emerging field wherein a single precursor can be utilized to produce different structural analogues. A number of methods have been reported for the synthesis of azapodophyllotoxin derivatives involving the multi-component reactions (MCRs) with aldehyde, amine and a cyclic diketone; though the nature of the aromatic amine is the prerequisite to this class of MCRs. However, some of the limitations have been observed for these methods including the reactivity of various amines, higher temperatures, long reaction times and the use of additives such as acetic acid, TFA, Et<sub>3</sub>N, and L-proline [26]. In 2015, Jeedimalla and co-workers successfully utilized various aromatic amines to access potent cytotoxic azapodophyllotoxin derivatives through a multi-component reaction [27]. More recently, Kandil and co-workers explored the commercially available 9-amino phenanthroline for the one-pot synthesis of phenanthroline based azapodophyllotoxin derivatives which displayed potent cytotoxicity [28]. In this context, we have attempted to explore the tetramethoxy phenanthrene amine as precursor for the one-pot synthesis of new cytotoxic phenanthrene fused-tetrahydrodibenzo-acridinones and we anticipate that these new hybrids may show enhanced cytotoxicity through apoptosis induction.

*<Insert Figure 1 here>*

## 2.0 Results and discussion

### 2.1 Chemistry

Phenanthrene fused-tetrahydrodibenzo-acridinones **8a–r** were synthesized by a one-pot method by involving 2,3,6,7-tetramethoxyphenanthren-9-amine (**5**), dimedone (**6a**) or

cyclohexane dione (**6b**) with various substituted aromatic aldehydes **7a–r** in refluxing EtOH under microwave irradiation as shown in **Scheme 1**. Initially, Knoevenagel condensation of cyclic diketone and aldehyde results in an intermediate which upon Michael addition with amine followed by subsequent cyclization affords the desired phenanthrene fused-dihydrodibenzo-quinolin-ones **8a–r**. Herein, we have utilized the microwave-irradiation technique to this one-pot process in order to increase the yields of the reaction and reduction of the reaction time. Gratifyingly, the microwave heating remarkably decreased the reaction time from 3 h (conventional heating) to 20 min (microwave) thus saving the time and increasing the yields up to 91% (entry 6, **Table 1**). Microwave irradiation at 150 °C for 20 min was the optimized reaction conditions which provided high reaction yields. Moreover, this reaction did not require any base or catalyst and the electron with-drawing, electron donating, heteroaromatic aldehydes and bicyclic aromatic aldehydes participated effectively in the reaction. In order to make the protocol further environmental friendly, we have also carried out the reaction in water, unfortunately the reaction did not proceed (entry 8, **Table 1**). This may be due to the low solubility of phenanthrene amine in water. The desired final products were collected by simple filtration followed by recrystallization and without using any column chromatographic purification. The key amine precursor **5** was synthesized from benzyl 2,3,6,7-tetramethoxyphenanthren-9-yl carbamate (**4**) in good yield as shown in **Scheme 1**. Compound **4** was obtained by using six steps sequence according to the reported procedure [29]. Initially, Perkin condensation of **2** with **1** affords 2,3-bis(3,4-dimethoxyphenyl)acrylic acid which was further esterified and then intramolecular oxidative cyclization with *m*-CPBA/TFA provides the corresponding ester **3**. Later, this ester functionality was converted to acyl hydrazide followed by diazotization using NaNO<sub>2</sub>/HCl-H<sub>2</sub>O affords the acyl azide as a key intermediate. Upon Curtius rearrangement reaction, the acyl azide is converted in to 2,3,6,7-tetramethoxyphenanthren-9-yl carbamate (**4**) in overall 67% yield. Finally, benzyl-carbamate was deprotected by using TBAF to get the tetramethoxy phenanthrene amine (**5**) as key precursor for this one-pot method. All the synthesized compounds (**8a–r**) were successfully characterized by <sup>1</sup>H, <sup>13</sup>C NMR spectroscopies and HRMS. The <sup>1</sup>H NMR of compound **8a** showed a sharp singlet of NH proton at δ 9.05 ppm. The two doublets 2.19 and 1.99 correspond to the methylenic protons adjacent to the dimethyl substitution. Protons of -CH<sub>2</sub>- which is adjacent to carbonyl group resonated as multiplet around 2.63 and 2.61 ppm. The two singlets of three protons each at δ 0.98 and 0.79 belong to the dimethyl groups of cyclic ketone of 'D' ring. Proton attached to tertiary carbon is detected as singlet at δ 5.65 ppm. Characteristic methoxy protons appeared

as a singlet at  $\delta$  3.95–3.74 ppm. Similarly, in  $^{13}\text{C}$  NMR spectrum of compound **8a**, the carbonyl carbon appeared at  $\delta$  193.8 ppm. The two methyl carbons resonated around  $\delta$  26.8 and 29.6 ppm. The signal such as two  $-\text{CH}_2-$  of the ‘D’ ring appeared at  $\delta$  36.8 and 50.6 ppm. Tertiary carbon showed a characteristic peak of  $\delta$  40.7 ppm and all the aromatic carbons resonates around  $\delta$  151.4–103.6 ppm. Similar pattern was observed in  $^1\text{H}$  NMR and  $^{13}\text{C}$  NMR of all the final compounds **8b–r**. The HRMS (ESI) of all the derivatives showed an  $[\text{M} + \text{H}]^+$  peak equivalent to their corresponding molecular formula.

<Insert Table 1 here>

<Insert Scheme 1 here>

## 2.2 Pharmacology

### 2.2.1 *In vitro* cytotoxicity study

The new phenanthrene fused-tetrahydrodibenzo-acridinone derivatives **8a–r** were tested for their *in vitro* cytotoxic potential against selected human cancer cell lines of cervical (HeLa), prostate (PC-3), fibro sarcoma (HT-1080), ovarian (SKOV-3) and also a normal (Hek-293T) kidney cell line by using 3-(4,5-dimethylthiazol-2-yl)-2,5-diphenyltetrazolium bromide (MTT) assay [30]. The  $\text{IC}_{50}$  ( $\mu\text{M}$ ) values (concentration required to inhibit 50% of the cancer cells) of the tested compounds and the positive control drug cisplatin are listed in **Table 2**. It was observed from the cytotoxicity results that derivatives **8l** and **8m** displayed potent cytotoxicity ( $< 1 \mu\text{M}$ ) against SKOV-3 ovarian cancer cell line with an  $\text{IC}_{50}$  value of  $0.61 \pm 0.08$  and  $0.24 \pm 0.05 \mu\text{M}$  respectively. The derivatives **8l** and **8m** were effective on all of the tested cancer cell lines below  $10 \mu\text{M}$ . In detailed analysis, majority of the compounds such as **8i**, **8k**, **8l**, **8m**, **8o**, **8q** and **8r** have showed significant cytotoxicity ( $< 10 \mu\text{M}$ ) on the entire tested cancer cell lines which are not having geminal methyl substitution in the hexocyclic ‘D’ ring. Interestingly, one compound **8h** having dimethyl substitution in ‘D’ ring and a syringal group (3,5-dimethoxy-4-hydroxy substitution) as ‘E’ ring displayed more cytotoxicity ( $< 10 \mu\text{M}$ ) on all cancer cells. All the new compounds were adequately active on fibrosarcoma (HT-1080) and ovarian (SKOV-3) cancer cell lines. Except derivatives **8a**, **8c**, **8d** and **8j**, remaining all derivatives was active on the cervical (HeLa) and prostate (PC-3) cancer cell lines. Compound **8m** with unsubstituted hexocyclic ‘D’ ring with a 3-trifluoromethyl phenyl as ‘E’ ring proved to be the best potent compound among all and displayed  $\text{IC}_{50}$  of  $0.24 \pm 0.05 \mu\text{M}$  against SKOV-3 ovarian cancer cell line thus indicating the crucial role of fluorine in binding to the biomolecular target. Compound **8i** with a 3,4-

methylene dioxy substitution on aromatic E ring was found to be active ( $< 10 \mu\text{M}$ ) on all the cancer cell lines with highest potency ( $\text{IC}_{50} 1.35 \pm 0.24 \mu\text{M}$ ) on HeLa (cervical cancer) cells. Compounds **8e**, **8h**, **8i**, **8k**, **8l**, **8n**, **8o**, **8q** and **8r** displayed cytotoxicity below  $10 \mu\text{M}$  against PC-3 prostate cancer cells, among them compound **8r** bearing bicyclic naphthyl 'E' ring being the most potent showed  $\text{IC}_{50} 5.31 \pm 0.23 \mu\text{M}$ . Further, cytotoxicity of all these compounds was evaluated on normal cell line Hek-293T (human embryonic kidney) to determine the selectivity index (ratio of cytotoxicity of normal cell line to that of cancer cell line) which is a prerequisite for a lead chemotherapeutic agent. All the tested compounds displayed lower cytotoxicities on normal kidney cells (Hek-293T) when compared to the cancer cells. Hence, the compounds are safer towards the normal cells. The most potent compound showed  $\text{IC}_{50}$  value of  $18.5 \pm 0.89 \mu\text{M}$  against (Hek-293T) and its selectivity index is approximately 77.0 against SKOV-3 ovarian cancer cells. After the careful analysis of cytotoxicity results, it could be observed that methyl substituted 'D' ring analogues are comparatively less potent than that of the derivatives with unsubstituted 'D' ring. On the other hand, phenyl 'E' ring is favourable compared to that of the bicyclic and heterocyclic 'E' ring. Bulky electron donating groups such as methoxy, methyl, dimethoxy and trimethoxy substitutions on the 'E' ring are more favourable and displayed a greater cytotoxicity when compared to the halogen (Br and Cl) containing derivatives. On the basis of all these observations, a general Structural Activity Relation (SAR) was established and presented in **Figure 2**. Based on the interesting cytotoxicity results, one of the potent compounds **8m** was carried to further studies in detail like cancer cell growth inhibition and apoptosis induction.

*<Insert Table 2 here>*

*<Insert Figure 2 here>*

### 2.2.2 Effect on F-actin polymerisation

Membrane protrusions are responsible for the motility of cancer cells. Polymerisation of actin filaments initiates the ordered arrangement of membrane protrusions and thereby triggers cancer cell motility and stress fibre assembly [31]. Hence, it is very important to study the effect of potent compound **8m** on stress fibre formation and F-actin polymerisation. The assembling of actin cytoskeleton in SKOV-3 cancer cells was studied by staining the cells with rhodamine phalloidin, a red fluorescent dye which specifically binds the F-actin proteins. SKOV-3 cells were treated with 0.1, 0.2 and  $0.5 \mu\text{M}$  of compound **8m** followed by staining with rhodamine-phalloidin. **Figure 3** clearly showed that control cells having

numerous F-actin extensions and stress fibres where as compound **8m** treatment led to the stress fibre disruption around the nucleus and F-actin extensions were also not prominent. This indicates that compound **8m** inhibits the migratory potential of SKOV-3 cancer cells by disrupting F-actin assembly.

<Insert Figure 3 here>

### 2.2.3 Cell cycle analysis

Majority of the chemotherapeutic agents display their growth inhibitory potential by arresting specific phase of the cell cycle [32]. Thus the blockade of cell cycle progression by cytotoxic agents has a crucial role to develop into a potential chemotherapeutic agent. From *in vitro* screening results, it is evident that compound **8m** displayed potent cytotoxicity against SKOV-3 ovarian cancer cells. Therefore, we studied the effect of compound **8m** on distribution of cells in various cell cycle phases by flow cytometric analysis [33]. SKOV-3 cells were treated with compound **8m** at 0.1, 0.2, and 0.5  $\mu\text{M}$ , for 24 h, and ethanol fixed cells were stained with propidium iodide and further subjected to flow cytometry. As observed from **Figure 4A** and **4B** the ratio of cells in G2/M phase from 14.7% in control raised to 22.6% at 0.1  $\mu\text{M}$ , 33.5% at 0.2  $\mu\text{M}$ , and 37.9% at 0.5  $\mu\text{M}$  and simultaneous decreased number of cells in G0/G1 phase. Therefore, these results clearly revealed that compound **8m** effectively exerts G2/M phase arrest on SKOV-3 cancer cells.

<Insert Figure 4 here>

### 2.2.4 Hoechst staining

Condensation of chromatin and DNA fragmentation are the important characteristics of apoptosis [34]. In order to know the apoptosis inducing ability of compound **8m** on SKOV-3 cells, Hoechst nuclear staining was performed. Hoechst 33242 is a nuclear staining dye which permeates through the cell wall and stains the live nucleus as light blue where as the apoptotic cells are stained bright blue due to the presence of condensed chromatin. SKOV-3 cells were stained by Hoechst 33242 followed by treatment with the compound **8m** at 0.1 , 0.2 and 0.5  $\mu\text{M}$ . Fluorescence microscope was used to observe the altered morphological changes in SKOV-3 cells. From **Figure 5**, it was clearly evident that control cells nuclei were intact whereas compound **8m** treated cells showed condensed chromatin, fragmented nuclei, pyknotic and horse shoe shaped nuclei indicating the progress of apoptosis.

<Insert Figure 5 here>

### 2.2.5 Mitochondrial membrane potential staining

Further to investigate the apoptosis inducing ability of the compound **8m**, mitochondrial membrane potential alterations were analysed by using a fluorescent probe JC-1. This is a lipophilic cationic dye that penetrates the cell membrane and accumulates in normally respiring mitochondria [35]. In the control cells, the JC-1 accumulates in mitochondria and stains high red fluorescence. However, in case of apoptotic cells, there is a collapsed mitochondrial potential. Therefore, JC-1 exists in cell cytosol as a monomer and emits green fluorescence. SKOV-3 cancer cells were treated with **8m** at concentrations of 0.1, 0.2, and 0.5  $\mu\text{M}$  respectively for 24 h and stained with JC-1 dye, untreated cells were used as control and the results were depicted in **Figure 6**.

The J-aggregates and JC-1 monomer were excited at 585 nm and 514 nm respectively and light emissions were recorded at 570-600 nm (red fluorescence) and 515-545 nm (green fluorescence). From fluorescence microscopy (**Figure 6**), it was clearly observed that control cells without compound **8m** were normally red, while **8m** treated cells showed strong green fluorescence that indicates typical apoptotic morphology after 24 h. Therefore, it was clearly evident from the JC-1 staining that active compound **8m** induced apoptosis in SKOV-3 cancer cells.

<Insert Figure 6 here>

### 2.2.6 Effect of **8m** on reactive oxygen species (ROS) levels

The increased levels of ROS in the mitochondrion may lead to the oxidative damage to the mitochondrial membrane and results in apoptosis [36]. Thus, we have used the DCFDA staining method to study the extent of apoptosis through ROS generation. Carboxy-2, 7-dichlorofluorescein diacetate (Carboxy- $\text{H}_2\text{DCFDA}$ ) dye which upon cleavage by intracellular esterases oxidizes to highly fluorescent carboxy-2, 7-dichlorofluorescein (Carboxy-DCF). This can be quantified by spectrofluorometer. As observed from **Figure 7**, increased ROS production was observed in **8m** treated cells that showed increased green fluorescence 128.5% at 0.1  $\mu\text{M}$ , 150.3% at 0.2  $\mu\text{M}$  and 204.76% at 0.5  $\mu\text{M}$  when compared to control (100%). Quantitative analysis by spectrofluorometry revealed that the ROS levels increased 2-times higher when compared to that of control cells. This study suggests that the cytotoxicity of compound also dependent on ROS production.

<Insert Figure 7 here>

### 2.2.7 Caspase-3 colorimetric assay

Apoptosis is a critical cellular process that regulates the balance between cell proliferation, growth arrest and cell death. Several chemotherapeutics have been established to induce apoptosis via a caspase-dependent pathway [37]. Caspases represent a family of cysteinyl aspartate specific proteases and are responsible for induction of apoptosis. Caspase-3 is an “effector” caspase associated with the initiation of cell death and is therefore an important marker of the cells entry in to an apoptotic cascade pathway. The caspase-3 activity on SKOV-3 cancer cells upon treating with **8m** was measured calorimetrically at an absorbance of 405 nm. As observed from **Figure 8**, caspase-3 activity (fold increase) was observed to be 1.58 at 0.1  $\mu\text{M}$ , 2.45 at 0.2  $\mu\text{M}$ , and 3.78 at 0.5  $\mu\text{M}$  respectively. Caspase activity in control cells considered as 1 and the caspase activity was increased to 3.7 folds at 0.5  $\mu\text{M}$  in comparison to control. Therefore, the results clearly revealed that compound **8m** effectively induced caspase mediated cell apoptosis in SKOV-3 cancer cells.

<Insert Figure 8 here>

### 2.2.8 Tumor spheroid growth inhibition

Mono layer culture cells are the most commonly used models to screen the antitumor activity of new drugs. However, this model is devoid of dense extracellular-matrix, three dimensionality, heterogeneity and penetration barriers observed *in vivo* in solid tumors. The use of three dimensional (3D) models has been assumed as an effective approach to overcome the limitations of the traditional two-dimensional (2D) systems. 3D spheroids are good mimics of *in vivo* tumor environment in *in vitro* study and provide more reliable information than 2D cultures [38]. In previous studies, we have studied the effectiveness of compound **8m** against SKOV-3 cells in 2D culture. Therefore, in order to know the potential effect of compound **8m** on solid tumors, we have developed 3D spheroids of SKOV-3 cancer cells and treated with compound at 0.1, 0.2 and 0.5  $\mu\text{M}$  concentrations for 72 h. From the **Figure 9**, it was quite interesting to observe that the spheroid forming capability of the cells treated with 0.5  $\mu\text{M}$  of active compound is suppressed to the great extent after 3 days (72 h).

<Insert Figure 9 here>

### 3.0 Conclusion

In summary, the present work demonstrates the microwave-assisted one-pot synthesis of phenanthrene fused-tetrahydrodibenzo-acridinone derivatives. The present synthetic strategy provided quick assembly of three different components in to a single complex molecule. This method also offered advantages like faster reaction times, high yields, wide substrate scope, atom-economy, and eliminates the chromatographic purification process. Moreover, ethanol was used as green solvent for this one-pot reaction. The synthesized compounds were evaluated for their *in vitro* cytotoxic potential against various selected human cancer cell lines and also a normal kidney cell line. From *in vitro* screening results, it was observed that compound **8m** displayed potent cytotoxicity against SKOV-3 ovarian cancer cells with an IC<sub>50</sub> value of 0.24±0.05 μM. Compound **8m** induced disruption of F-actin filaments and inhibited cancer cell motility. Flow cytometric analysis indicated that the compound blocked the G2/M phase of the cell cycle. Moreover, the compound also leads to decrease in the number of viable cells and increased apoptotic features as shown in case of Hoechst staining. **8m** also caused the collapse of mitochondrial membrane potential as evident from JC-1 staining and also enhanced the generation of reactive oxygen species. The compound has increased the caspase-3 activation by 3.7 fold thereby supporting the strong apoptosis. Moreover, **8m** has greatly reduced the *in vitro* 3D-spheroid inhibition in SKOV-3 ovarian cancer cells. Overall, all the studies indicated that these compounds are potentially inhibiting the ovarian cancer cells and may be developed as potent chemotherapeutic agents for the treatment of malignancies in the drug discovery.

### 4.0 Experimental protocols

#### 4.1 Chemistry

All reagents and solvents were obtained from commercial suppliers and were used without further purification. Analytical thin layer chromatography (TLC) was performed on MERCK precoated silica gel 60-F<sub>254</sub> (0.5 mm) aluminum plates. Visualization of the spots on TLC plates was achieved by UV light. <sup>1</sup>H and <sup>13</sup>C NMR spectra were recorded on Bruker 500 MHz. Making a solution of samples in CDCl<sub>3</sub> solvent is using tetramethyl silane (TMS) as the internal standard. Chemical shifts for <sup>1</sup>H and <sup>13</sup>C are reported in parts per million (ppm) downfield from tetra methyl silane. Spin multiplicities are described as s (singlet), bs (broad singlet), d (doublet), dd (double doublet), t (triplet), q (quartet), and m (multiplet). Coupling constant (*J*) values are reported in hertz (Hz). HRMS were determined with Agilent QTOF

mass spectrometer 6540 series instrument. Wherever required, column chromatography was performed using silica gel (60-120 or 100-200) or neutral alumina. The reactions wherever anhydrous conditions required are carried under nitrogen positive pressure using freshly distilled solvents. All evaporation of solvents was carried out under reduced pressure on Heidolph rotary evaporator below 45 °C.

#### 4.1.1 General reaction procedure for the synthesis of phenanthrene fused-tetrahydrodibenzo-acridinones **8a–r**

A mixture of 2,3,6,7-tetramethoxy phenanthrene-9-amine (**5**, 0.28 mmol), cyclohexane dione (**6a**, 0.28 mmol) or dimethyl cyclo hexane dione (**6b**, 0.28 mmol) and substituted aldehydes (**7a–r**, 0.28 mmol) in EtOH (3 mL) were heated through microwave irradiation at 150 °C for 0.3 h. After completion of the reaction, the reaction mixture was allowed to cool to room temperature and the precipitated products were collected by vacuum filtration and washed with water followed by recrystallization from ethanol to afford pure compounds **8a–r** in 89-95% yields. All the synthesized compounds were thoroughly characterized by <sup>1</sup>H NMR, <sup>13</sup>C NMR and HRMS (ESI).

##### 4.1.1.1 Microwave irradiation experiments

Microwave irradiation was carried out in a monowave 300 single-mode microwave reactor from Anton paar GmbH (Graz, Austria). The reaction temperature was monitored by an external infra red (IR) sensor housed in the side walls of the microwave cavity measuring the surface temperature of the reaction vessel. Reaction times refer to the hold time at the desired set temperature and not to the total irradiation time. Reusable 10 mL G10 pyrex vials were sealed with PEEK snap caps and standard PTFE coated silicone septa. Reaction cooling was achieved by compressed air automatically after the heating period has elapsed.

##### 4.1.1.2 14-(4-Chlorophenyl)-2,3,6,7-tetramethoxy-11,11-dimethyl-10,11,12,14-tetrahydrodibenzo[*a,c*]acridin-13(9H)-one (**8a**)

White solid, yield 92%; mp: 273–275 °C; <sup>1</sup>H NMR (500 MHz, DMSO-*d*<sub>6</sub>): δ 9.05 (s, 1H), 7.93 (s, 1H), 7.87 (s, 1H), 7.78 (s, 1H), 7.20 (t, *J* = 8.08 Hz, 3H), 7.12 (d, *J* = 7.93 Hz, 2H), 5.65 (s, 1H), 3.95 (s, 6H), 3.87 (s, 3H), 3.74 (s, 3H), 2.63–2.61 (m, 2H), 2.19 (d, *J* = 16.02 Hz, 1H), 1.99 (d, *J* = 15.86 Hz, 1H), 0.98 (s, 3H), 0.79 (s, 3H) ppm; <sup>13</sup>C NMR (125 MHz, DMSO-*d*<sub>6</sub>): δ 193.8, 151.4, 149.6, 149.4, 149.1, 147.9, 146.4, 130.4, 130.0, 128.7, 128.2, 124.7, 124.6, 122.1, 117.2, 112.8, 107.8, 105.2, 104.8, 104.5, 103.6, 56.7, 56.4, 56.3, 55.7,

50.6, 40.7, 36.8, 32.6, 29.6, 26.8 ppm; HRMS (ESI):  $m/z$  calcd for  $C_{33}H_{32}ClNO_5$  558.2042, found 558.2050  $[M+H]^+$ .

4.1.1.3 *14-(3,4-Dimethoxyphenyl)-2,3,6,7-tetramethoxy-11,11-dimethyl-10,11,12,14-tetrahydrodibenzo[a,c]acridin-13(9H)-one (8b)*

Yellow solid, yield 90%; mp:  $> 300^\circ\text{C}$ ;  $^1\text{H}$  NMR (500 MHz,  $\text{DMSO}-d_6$ ):  $\delta$  9.09 (s, 1H), 8.01 (s, 1H), 7.95 (s, 1H), 7.86 (s, 1H), 7.39 (s, 1H), 7.04 (s, 1H), 6.69 (t,  $J = 8.54$  Hz, 2H), 5.66 (s, 1H), 4.03 (s, 6H), 3.96 (s, 3H), 3.85 (s, 3H), 3.62 (d,  $J = 13.42$  Hz, 6H), 2.74–2.65 (m, 2H), 2.27 (d,  $J = 16.02$  Hz, 1H), 2.08 (d,  $J = 15.86$  Hz, 1H), 1.07 (s, 3H), 0.91 (s, 3H) ppm;  $^{13}\text{C}$  NMR (125 MHz,  $\text{DMSO}-d_6$ ):  $\delta$  193.9, 150.9, 149.4, 149.3, 149.1, 148.4, 147.8, 147.2, 140.4, 128.4, 124.9, 124.6, 122.1, 120.3, 117.2, 113.6, 112.8, 111.8, 108.5, 105.1, 104.9, 104.7, 103.4, 56.6, 56.5, 56.4, 56.3, 55.9, 55.8, 55.7, 50.7, 36.7, 32.6, 29.7, 26.8 ppm; HRMS (ESI):  $m/z$  calcd for  $C_{35}H_{37}NO_7$  584.2643, found 584.2657  $[M+H]^+$ .

4.1.1.4 *2,3,6,7-Tetramethoxy-11,11-dimethyl-14-(4-(trifluoromethyl)phenyl)-10,11,12,14-tetrahydrodibenzo[a,c]acridin-13(9H)-one (8c)*

Off white solid, yield 92%; mp:  $186\text{--}188^\circ\text{C}$ ;  $^1\text{H}$  NMR (500 MHz,  $\text{DMSO}-d_6$ ):  $\delta$  9.19 (s, 1H), 8.02 (s, 1H), 7.96 (s, 1H), 7.89 (s, 1H), 7.52 (s, 4H), 7.29 (s, 1H), 5.84 (s, 1H), 4.04 (s, 6H), 3.96 (s, 3H), 3.83 (s, 3H), 2.74–2.69 (m, 2H), 2.28 (d,  $J = 15.86$  Hz, 1H), 2.08 (d,  $J = 16.02$  Hz, 1H), 1.08 (s, 3H), 0.87 (s, 3H) ppm;  $^{13}\text{C}$  NMR (125 MHz,  $\text{DMSO}-d_6$ ):  $\delta$  193.8, 151.8, 151.5, 149.6, 149.4, 149.2, 147.9, 129.0, 128.7, 126.8, 126.5, 125.8, 125.3, 124.8, 124.5, 123.7, 122.1, 117.0, 112.5, 107.5, 105.1, 104.9, 104.4, 103.5, 56.7, 56.4, 56.3, 55.7, 50.6, 37.5, 32.7, 29.5, 26.8 ppm; HRMS (ESI):  $m/z$  calcd for  $C_{34}H_{32}F_3NO_5$  592.2305, found 592.2312  $[M+H]^+$ .

4.1.1.5 *14-(4-Isopropylphenyl)-2,3,6,7-tetramethoxy-11,11-dimethyl-10,11,12,14-tetrahydrodibenzo[a,c]acridin-13(9H)-one (8d)*

Brown solid, yield 95%; mp:  $175\text{--}177^\circ\text{C}$ ;  $^1\text{H}$  NMR (500 MHz,  $\text{DMSO}-d_6$ ):  $\delta$  9.09 (s, 1H), 8.01 (s, 1H), 7.95 (s, 1H), 7.87 (s, 1H), 7.39 (s, 1H), 7.23 (d,  $J = 8.24$  Hz, 2H), 7.00 (d,  $J = 8.08$  Hz, 2H), 5.68 (s, 1H), 4.04 (d,  $J = 2.13$  Hz, 6H), 3.96 (s, 3H), 3.85 (s, 3H), 2.74–2.69 (m, 3H), 2.25 (d,  $J = 16.02$  Hz, 1H), 2.09 (d,  $J = 16.02$  Hz, 1H), 1.07 (d,  $J = 6.25$  Hz, 9H), 0.92 (s, 3H) ppm;  $^{13}\text{C}$  NMR (125 MHz,  $\text{DMSO}-d_6$ ):  $\delta$  193.8, 151.1, 149.5, 149.4, 149.0, 147.8, 145.8, 145.1, 128.4, 128.2, 126.1, 124.8, 124.5, 122.1, 117.2, 113.6, 108.4, 105.1,

104.8, 104.7, 103.4, 56.6, 56.4, 56.3, 55.7, 50.7, 40.8, 36.8, 33.3, 32.7, 29.5, 27.2, 24.3, 24.1 ppm; HRMS (ESI):  $m/z$  calcd for  $C_{36}H_{39}NO_5$  566.2901, found 566.2906  $[M+H]^+$ .

4.1.1.6 *2,3,6,7-Tetramethoxy-11,11-dimethyl-14-(3,4,5-trimethoxyphenyl)-10,11,12,14-tetrahydrodibenzo[a,c]acridin-13(9H)-one (8e)*

Brown solid, yield 90%; mp: 254–256 °C;  $^1H$  NMR (500 MHz,  $DMSO-d_6$ ):  $\delta$  9.15 (s, 1H), 8.02 (s, 1H), 7.97 (s, 1H), 7.86 (s, 1H), 7.44 (s, 1H), 6.63 (s, 2H), 5.67 (s, 1H), 4.04 (d,  $J = 4.57$  Hz, 6H), 3.97 (s, 3H), 3.89 (s, 3H), 3.59 (s, 6H), 3.53 (s, 3H), 2.74–2.70 (m, 2H), 2.24 (d,  $J = 16.02$  Hz, 1H), 2.11 (d,  $J = 16.02$  Hz, 1H), 1.08 (s, 3H), 0.95 (s, 3H) ppm;  $^{13}C$  NMR (125 MHz,  $DMSO-d_6$ ):  $\delta$  193.9, 152.7, 151.2, 149.5, 149.3, 149.1, 147.9, 143.5, 136.1, 128.4, 124.9, 124.6, 122.1, 117.2, 113.5, 108.3, 106.0, 105.1, 104.8, 104.7, 103.4, 60.3, 56.6, 56.4, 56.3, 56.2, 55.7, 50.7, 40.8, 37.5, 32.7, 29.7, 35.7 ppm; HRMS (ESI):  $m/z$  calcd for  $C_{36}H_{39}NO_8$  614.2748, found 614.2761  $[M+H]^+$ .

4.1.1.7 *14-(4-Bromophenyl)-2,3,6,7-tetramethoxy-11,11-dimethyl-10,11,12,14-tetrahydrodibenzo[a,c]acridin-13(9H)-one (8f)*

White solid, yield 94%; mp: 193–195 °C;  $^1H$  NMR (500 MHz,  $CDCl_3$ ):  $\delta$  7.83 (s, 1H), 7.72 (s, 1H), 7.30 (s, 1H), 7.26–7.21 (m, 5H), 5.86 (s, 1H), 4.12 (d,  $J = 7.01$  Hz, 6H), 4.04 (s, 3H), 3.89 (s, 3H), 2.56–2.52 (m, 2H), 2.34–2.24 (m, 2H), 1.10 (s, 3H), 0.94 (s, 3H) ppm;  $^{13}C$  NMR (125 MHz,  $CDCl_3$ ):  $\delta$  194.8, 150.0, 149.3, 149.2, 147.9, 145.2, 131.1, 129.8, 127.2, 124.8, 122.1, 119.7, 116.3, 113.5, 109.1, 104.6, 104.0, 103.5, 100.7, 56.3, 56.1, 55.7, 50.5, 42.0, 37.0, 32.7, 29.4, 27.0 ppm; HRMS (ESI):  $m/z$  calcd for  $C_{33}H_{32}BrNO_5$  602.1537, found 602.1541  $[M+H]^+$ .

4.1.1.8 *14-(4-Hydroxy-3-methoxyphenyl)-2,3,6,7-tetramethoxy-11,11-dimethyl-10,11,12,14-tetrahydrodibenzo[a,c]acridin-13(9H)-one (8g)*

Yellow solid, yield 91%; mp: 285–287 °C;  $^1H$  NMR (500 MHz,  $CDCl_3$ ):  $\delta$  7.87 (s, 1H), 7.75 (s, 1H), 7.45 (s, 1H), 7.20 (s, 1H), 7.11 (s, 1H), 6.95 (Brs, 1H), 6.69 (dd,  $J = 7.93, 24.26$  Hz, 2H), 5.87 (s, 1H), 5.45 (Brs, 1H), 4.14 (d,  $J = 9.91$  Hz, 6H), 4.07 (s, 3H), 3.94 (s, 3H), 3.78 (s, 3H), 2.56 (s, 2H), 2.35–2.27 (m, 2H), 1.12 (s, 3H), 0.99 (s, 3H) ppm;  $^{13}C$  NMR (125 MHz,  $CDCl_3$ ):  $\delta$  195.2, 149.3, 149.2, 149.1, 149.0, 147.8, 146.0, 143.5, 138.6, 127.1, 125.2, 124.7, 122.0, 120.7, 116.3, 114.2, 114.0, 111.2, 110.1, 105.0, 104.2, 103.5, 100.3, 56.3, 56.1, 55.8, 55.7, 50.8, 42.2, 36.8, 32.7, 29.6, 29.4, 27.1 ppm; HRMS (ESI):  $m/z$  calcd for

$C_{34}H_{35}NO_7$  570.2486, found 570.2492  $[M+H]^+$ .

4.1.1.9 *14-(4-Hydroxy-3,5-dimethoxyphenyl)-2,3,6,7-tetramethoxy-11,11-dimethyl-10,11,12,14-tetrahydrodibenzo[a,c]acridin-13(9H)-one (8h)*

Yellow solid, yield 90%; mp: 216–218 °C;  $^1H$  NMR (500 MHz,  $CDCl_3$ ):  $\delta$  7.78 (s, 1H), 7.67 (s, 1H), 7.37 (s, 1H), 7.13 (s, 1H), 6.92 (Brs, 1H), 6.54 (s, 2H), 5.78 (s, 1H), 4.06 (d,  $J = 7.62$  Hz, 6H), 3.98 (s, 3H), 3.86 (s, 3H), 3.61 (s, 6H), 2.48 (s, 2H), 2.22–2.10 (m, 2H), 1.02 (s, 3H), 0.91 (s, 3H) ppm;  $^{13}C$  NMR (125 MHz,  $CDCl_3$ ):  $\delta$  195.1, 149.3, 149.2, 149.1, 149.0, 147.9, 146.7, 137.7, 132.9, 127.1, 125.3, 124.8, 122.0, 116.2, 114.0, 109.9, 105.3, 105.0, 104.2, 103.5, 100.4, 56.3, 56.2, 56.1, 56.0, 55.7, 50.7, 42.2, 37.2, 32.7, 29.4, 26.9 ppm; HRMS (ESI):  $m/z$  calcd for  $C_{35}H_{37}NO_8$  600.2592, found 600.2598  $[M+H]^+$ .

4.1.1.10 *14-(Benzo[d][1,3]dioxol-5-yl)-2,3,6,7-tetramethoxy-11,11-dimethyl-10,11,12,14-tetrahydrodibenzo[a,c]acridin-13(9H)-one (8i)*

Off white solid, yield 89%; mp: 201–203 °C;  $^1H$  NMR (500 MHz,  $DMSO-d_6$ ):  $\delta$  9.10 (s, 1H), 8.01 (s, 1H), 7.96 (s, 1H), 7.86 (s, 1H), 7.34 (s, 1H), 6.78 (s, 1H), 6.75 (d,  $J = 8.08$  Hz, 1H), 6.67 (d,  $J = 8.08$  Hz, 1H), 5.87 (s, 1H), 5.82 (s, 1H), 5.67 (s, 1H), 4.04 (d,  $J = 1.83$  Hz, 6H), 3.96 (s, 3H), 3.84 (s, 3H), 2.72–2.68 (m, 2H), 2.26 (d,  $J = 16.02$  Hz, 1H), 2.10 (d,  $J = 15.86$  Hz, 1H), 1.07 (s, 3H), 0.91 (s, 3H) ppm;  $^{13}C$  NMR (125 MHz,  $DMSO-d_6$ ):  $\delta$  194.0, 151.1, 149.5, 149.4, 149.1, 147.9, 147.2, 145.3, 141.7, 128.5, 124.7, 124.6, 122.1, 121.1, 117.1, 113.4, 108.5, 108.3, 108.0, 105.1, 104.8, 104.7, 103.4, 101.0, 56.6, 56.4, 56.3, 55.7, 50.7, 40.7, 36.8, 32.6, 29.6, 26.9 ppm; HRMS (ESI):  $m/z$  calcd for  $C_{34}H_{33}NO_7$  568.2330, found 568.2334  $[M+H]^+$ .

4.1.1.11 *14-(3,4-Dimethoxyphenyl)-2,3,6,7-tetramethoxy-10,11,12,14-tetrahydrodibenzo[a,c]acridin-13(9H)-one (8j)*

Yellow solid, yield 92%; mp: 265–267 °C;  $^1H$  NMR (500 MHz,  $CDCl_3$ ):  $\delta$  7.86 (s, 1H), 7.73 (s, 1H), 7.40 (s, 1H), 7.20 (s, 1H), 7.12 (d,  $J = 1.52$  Hz, 1H), 6.99 (s, 1H), 6.73–6.71 (m, 1H), 6.58 (d,  $J = 8.39$  Hz, 1H), 5.92 (s, 1H), 4.13 (s, 3H), 4.09 (s, 3H), 4.05 (s, 3H), 3.90 (s, 3H), 3.76 (s, 3H), 3.72 (s, 3H), 2.70 (s, 2H), 2.51–2.37 (m, 2H), 2.04–2.03 (m, 2H) ppm;  $^{13}C$  NMR (125 MHz,  $CDCl_3$ ):  $\delta$  195.3, 151.1, 149.2, 149.1, 148.5, 147.8, 147.0, 139.5, 127.2, 125.2, 124.8, 122.0, 120.1, 116.3, 114.1, 112.0, 111.2, 110.8, 105.0, 104.1, 103.4, 100.6, 56.4, 56.1, 55.9, 55.7, 55.6, 37.0, 36.7, 28.5, 21.1 ppm; HRMS (ESI):  $m/z$  calcd for

$C_{33}H_{33}NO_7$  556.2330, found 556.2330  $[M+H]^+$ .

4.1.1.12 *2,3,6,7-Tetramethoxy-14-(p-tolyl)-10,11,12,14-tetrahydrodibenzo[a,c]acridin-13(9H)-one (8k)*

Yellow solid, yield 89%; mp: 290–292 °C;  $^1H$  NMR (500 MHz,  $CDCl_3$ ):  $\delta$  7.84 (s, 1H), 7.71 (s, 1H), 7.41 (s, 1H), 7.27 (s, 1H), 7.25 (s, 1H), 7.15 (Brs, 1H), 6.92 (d,  $J = 7.78$  Hz, 2H), 5.91 (s, 1H), 4.12 (s, 3H), 4.09 (s, 3H), 4.03 (s, 3H), 3.89 (s, 3H), 2.72 (s, 2H), 2.49–2.35 (m, 2H), 2.17 (s, 3H), 2.02 (s, 2H) ppm;  $^{13}C$  NMR (125 MHz,  $CDCl_3$ ):  $\delta$  195.1, 151.7, 149.2, 149.1, 147.8, 143.7, 135.3, 128.8, 128.1, 127.1, 125.1, 124.7, 122.1, 116.4, 114.5, 111.2, 104.9, 104.0, 103.4, 100.9, 56.4, 56.0, 55.7, 37.0, 36.9, 28.4, 21.1, 20.9 ppm; HRMS (ESI):  $m/z$  calcd for  $C_{32}H_{31}NO_5$  510.2275, found 510.2275  $[M+H]^+$ .

4.1.1.13 *2,3,6,7-Tetramethoxy-14-(4-methoxyphenyl)-10,11,12,14-tetrahydrodibenzo[a,c]acridin-13(9H)-one (8l)*

Off white solid, yield 90%; mp: > 300 °C;  $^1H$  NMR (500 MHz,  $CDCl_3$ ):  $\delta$  7.84 (s, 1H), 7.72 (s, 1H), 7.40 (s, 1H), 7.29 (s, 1H), 7.27 (s, 1H), 7.24 (s, 1H), 7.09 (s, 1H), 6.65 (d,  $J = 8.69$  Hz, 2H), 5.90 (s, 1H), 4.12 (s, 3H), 4.09 (s, 3H), 4.04 (s, 3H), 3.89 (s, 3H), 3.65 (s, 3H), 2.71–2.66 (m, 2H), 2.49–2.39 (m, 2H), 2.04–1.99 (m, 2H) ppm;  $^{13}C$  NMR (125 MHz,  $CDCl_3$ ):  $\delta$  193.8, 156.3, 151.8, 148.0, 147.9, 147.7, 146.4, 138.7, 128.0, 127.2, 123.9, 123.4, 120.9, 116.2, 112.9, 112.2, 109.1, 103.7, 102.7, 102.6, 102.4, 102.3, 55.7, 55.1, 55.0, 54.6, 53.9, 36.0, 35.2, 26.5, 20.2 ppm; HRMS (ESI):  $m/z$  calcd for  $C_{32}H_{31}NO_6$  526.2224, found 526.2227  $[M+H]^+$ .

4.1.1.14 *2,3,6,7-Tetramethoxy-14-(3-(trifluoromethyl)phenyl)-10,11,12,14-tetrahydrodibenzo[a,c]acridin-13(9H)-one (8m)*

Yellow solid, yield 90%; mp: 279–281 °C;  $^1H$  NMR (500 MHz,  $CDCl_3$ ):  $\delta$  7.84 (s, 1H), 7.72 (s, 1H), 7.69 (s, 1H), 7.56 (d,  $J = 7.62$  Hz, 1H), 7.31 (d,  $J = 10.68$  Hz, 2H), 7.25–7.21 (m, 2H), 5.99 (s, 1H), 4.12 (s, 3H), 4.10 (s, 3H), 4.04 (s, 3H), 3.89 (s, 3H), 2.76–2.71 (m, 2H), 2.49–2.40 (m, 2H), 2.07–1.99 (m, 2H) ppm;  $^{13}C$  NMR (125 MHz,  $CDCl_3$ ):  $\delta$  194.8, 152.9, 149.1, 148.9, 148.7, 148.0, 147.4, 131.6, 129.8, 129.5, 128.4, 128.2, 125.2, 124.7, 124.6, 124.6, 124.5, 123.0, 122.4, 122.3, 121.9, 116.9, 112.9, 109.4, 104.3, 103.5, 103.4, 103.1, 56.6, 55.9, 55.9, 55.4, 37.3, 36.8, 27.6, 21.0 ppm; HRMS (ESI):  $m/z$  calcd for  $C_{32}H_{28}F_3NO_5$  564.1992, found 564.1998  $[M+H]^+$ .

4.1.1.15 *14-(4-Isopropylphenyl)-2,3,6,7-tetramethoxy-10,11,12,14-tetrahydrodibenzo[a,c]acridin-13(9H)-one (8n)*

Light green solid, yield 91%; mp: 199–201 °C; <sup>1</sup>H NMR (500 MHz, CDCl<sub>3</sub>): δ 7.84 (s, 1H), 7.72 (s, 1H), 7.43 (s, 1H), 7.28 (d, *J* = 8.08 Hz, 2H), 7.24 (s, 1H), 7.12 (s, 1H), 6.95 (d, *J* = 8.69 Hz, 2H), 5.92 (s, 1H), 4.12 (s, 3H), 4.08 (s, 3H), 4.04 (s, 3H), 3.89 (s, 3H), 2.75–2.70 (m, 3H), 2.49–2.36 (m, 2H), 2.02–2.01 (m, 2H), 1.11 (dd, *J* = 2.28, 6.86 Hz, 6H), ppm; <sup>13</sup>C NMR (125 MHz, CDCl<sub>3</sub>): δ 195.4, 151.6, 149.1, 149.0, 147.7, 146.1, 144.0, 128.0, 127.2, 126.1, 125.2, 124.7, 122.0, 116.6, 114.5, 111.1, 105.1, 104.0, 103.3, 101.0, 56.3, 56.1, 56.0, 55.7, 37.1, 37.0, 33.5, 28.3, 23.8, 21.1 ppm; HRMS (ESI): *m/z* calcd for C<sub>34</sub>H<sub>35</sub>NO<sub>5</sub> 538.2588, found 538.2592 [M+H]<sup>+</sup>.

4.1.1.16 *2,3,6,7-Tetramethoxy-11,11-dimethyl-14-(thiophen-2-yl)-10,11,12,14-tetrahydrodibenzo[a,c]acridin-13(9H)-one (8o)*

Brown solid, yield 92%; mp: 270–272 °C; <sup>1</sup>H NMR (500 MHz, CDCl<sub>3</sub>): δ 7.86 (s, 1H), 7.77 (s, 1H), 7.48 (s, 1H), 7.25 (s, 1H), 6.96 (d, *J* = 4.57 Hz, 1H), 6.77 (s, 1H), 6.73 (t, *J* = 3.96 Hz, 1H), 6.26 (s, 1H), 4.14 (s, 3H), 4.08 (s, 6H), 3.94 (s, 3H), 2.61–2.57 (m, 2H), 2.54–2.37 (m, 2H), 1.12 (s, 3H), 1.04 (s, 3H) ppm; <sup>13</sup>C NMR (125 MHz, CDCl<sub>3</sub>): δ 194.7, 150.2, 150.0, 149.4, 149.3, 149.1, 148.0, 127.0, 126.2, 125.0, 124.8, 124.0, 123.4, 122.0, 116.3, 113.6, 109.0, 104.6, 104.0, 103.4, 100.7, 56.3, 56.1, 55.9, 50.5, 42.0, 32.7, 32.0, 29.5, 27.1 ppm; HRMS (ESI): *m/z* calcd for C<sub>31</sub>H<sub>31</sub>NO<sub>5</sub>S 530.1996, found 530.2005 [M+H]<sup>+</sup>.

4.1.1.17 *2,3,6,7-Tetramethoxy-11,11-dimethyl-14-(3-methylthiophen-2-yl)-10,11,12,14-tetrahydrodibenzo[a,c]acridin-13(9H)-one (8p)*

Off white solid, yield 92%; mp: > 300 °C; <sup>1</sup>H NMR (500 MHz, CDCl<sub>3</sub>): δ 7.83 (s, 1H), 7.75 (s, 1H), 7.42 (s, 1H), 7.25 (s, 1H), 6.86 (d, *J* = 5.03 Hz, 1H), 6.61 (d, *J* = 5.03 Hz, 1H), 6.17 (s, 1H), 4.14–4.09 (m, 6H), 4.07 (s, 3H), 4.04 (s, 3H), 2.63 (s, 3H), 2.57 (s, 2H), 2.38–2.29 (m, 2H), 1.11 (s, 3H), 1.02 (s, 3H) ppm; <sup>13</sup>C NMR (125 MHz, CDCl<sub>3</sub>): δ 194.7, 149.4, 149.3, 149.2, 149.1, 147.9, 145.2, 131.4, 129.4, 126.6, 125.0, 124.7, 122.2, 122.0, 116.3, 114.8, 109.2, 104.2, 104.0, 103.6, 100.7, 56.3, 56.2, 56.1, 56.0, 42.1, 32.6, 30.8, 29.5, 27.0, 14.6 ppm; HRMS (ESI): *m/z* calcd for C<sub>32</sub>H<sub>33</sub>NO<sub>5</sub>S 544.2152, found 544.2219 [M+H]<sup>+</sup>.

4.1.1.18 *2,3,6,7-Tetramethoxy-14-(thiophen-2-yl)-10,11,12,14-tetrahydrodibenzo[a,c]acridin-13(9H)-one (8q)*

Off white solid, yield 93%; mp: 258–260 °C; <sup>1</sup>H NMR (500 MHz, CDCl<sub>3</sub>): δ 7.84 (s, 1H), 7.75 (s, 1H), 7.45 (s, 1H), 7.33 (s, 1H), 6.95 (d, *J* = 4.73 Hz, 1H), 6.74–6.70 (m, 2H), 6.26 (s, 1H), 4.12 (s, 3H), 4.06 (Brs, 6H), 3.92 (s, 3H), 2.74–2.71 (m, 2H), 2.57–2.53 (m, 1H), 2.45–2.43 (m, 1H), 2.06 (s, 2H) ppm; <sup>13</sup>C NMR (125 MHz, CDCl<sub>3</sub>): δ 195.1, 151.8, 150.4, 149.3, 149.2, 149.1, 147.9, 127.0, 126.2, 125.0, 124.8, 124.1, 123.5, 122.0, 116.3, 113.6, 110.3, 104.6, 104.0, 103.4, 100.8, 56.3, 56.0, 55.9, 36.9, 31.9, 28.3, 21.2 ppm; HRMS (ESI): *m/z* calcd for C<sub>29</sub>H<sub>27</sub>NO<sub>5</sub> 502.1683, found 502.1685 [M+H]<sup>+</sup>.

4.1.1.19 *2,3,6,7-Tetramethoxy-14-(naphthalen-1-yl)-10,11,12,14-tetrahydrodibenzo[a,c]acridin-13(9H)-one (8r)*

Yellow solid, yield 89%; mp: 284–286 °C; <sup>1</sup>H NMR (500 MHz, CDCl<sub>3</sub>): δ 9.53 (s, 1H), 7.82 (s, 1H), 7.75 (d, *J* = 8.08 Hz, 1H), 7.66 (d, *J* = 10.98 Hz, 2H), 7.55 (d, *J* = 7.93 Hz, 1H), 7.42 (t, *J* = 7.47 Hz, 1H), 7.34 (d, *J* = 7.01 Hz, 1H), 7.28 (s, 1H), 7.24 (s, 2H), 7.15 (t, *J* = 7.62 Hz, 1H), 6.65 (s, 1H), 4.11 (s, 3H), 4.06 (s, 3H), 3.97 (s, 3H), 3.39 (s, 3H), 2.70 (s, 2H), 2.41–2.32 (m, 2H), 1.97–1.91 (m, 2H) ppm; <sup>13</sup>C NMR (125 MHz, CDCl<sub>3</sub>): δ 195.6, 150.8, 149.2, 149.1, 149.0, 147.6, 145.3, 133.3, 130.8, 128.4, 127.5, 126.9, 126.8, 126.1, 125.8, 125.5, 125.3, 125.2, 124.6, 121.8, 116.8, 116.4, 112.1, 105.1, 104.1, 103.3, 100.6, 56.3, 56.1, 56.0, 55.8, 37.0, 32.7, 28.7, 20.9 ppm; HRMS (ESI): *m/z* calcd for C<sub>35</sub>H<sub>31</sub>NO<sub>5</sub> 546.2275, found 546.2278 [M+H]<sup>+</sup>.

## 4.2 Biology

### 4.2.1. Cell Cultures

Cervical (HeLa), prostate (PC-3), fibrosarcoma (HT-1080), ovarian (SKOV-3) and normal kidney cells (HeK-293T) were procured from ATCC (American Type Cell culture Collection), Maryland USA and were grown in suitable DMEM (Dulbecco modified Eagle medium, Sigma), RPMI (Rosewell Park Memorial Institute, Sigma) supplemented with 10% foetal bovine serum with 1X stabilized antibiotic-antimycotic solution (Sigma) in a CO<sub>2</sub> incubator at 37 °C with 5% CO<sub>2</sub> and 90% relative humidity. Cells were treated with 0.05% trypsin/1mM EDTA solution for further passage.

### 4.2.2 In vitro cytotoxic activity

MTT reduction assay was performed to determine the cytotoxicity for all the new compounds **8a-r**. 3x10<sup>4</sup> cells per well were seeded in 100 μL respective media, supplemented with 10%

FBS in each well of 96-well microculture plates and incubated at 37 °C for 24 h, in a CO<sub>2</sub> incubator. Samples were diluted to the required concentrations in culture medium, were added to the wells with respective vehicle control. After incubating for 48 h, 100 µL MTT (3-(4,5-dimethylthiazol-2-yl)-2,5-diphenyl tetrazolium bromide) (5 mg/mL) was added to all the plates and allowed for 4 h incubation in dark. After 4h of incubation period, the MTT media was removed and DMSO (100 µL) was added to each well to dissolve the formazan crystals. The absorbance was recorded on a micro-plate reader at 570 nm wavelength and at a reference wave length of 630 nm. The % inhibition was calculated as  $100 - [(Mean\ OD\ of\ treated\ cells \times 100) / Mean\ OD\ of\ vehicle\ treated\ cells\ (DMSO)]$ . All the experiments and IC<sub>50</sub> values were computed by using Probit Software.

#### 4.2.3 *F-actin staining*

SKOV-3 cells ( $1 \times 10^6$  cells/well) were grown on cover slips in 6 well plates for 24 h and then incubated with 0.1 µM, 0.2 µM and 0.5 µM of compound **8m** for 24 h. After the compound treatment, cells were washed with PBS and fixed with 4% para-formaldehyde in PBS. Cells were incubated with rhodamine-phalloidin for actin staining and Hoechst 33242 for nucleus staining. After washing thrice with PBS, cells were mounted with ProLong Gold anti-fade reagent (Molecular Probes, Eugene, OR) on microscopic slide and were visualized by confocal fluorescence microscopy (Nikon). Images were captured using 20X magnification objective lenses.

#### 4.2.4 *Cell cycle analysis*

SKOV-3 cells ( $1 \times 10^6$  cells/well) in 6 well plate were treated with 0.1 µM, 0.2 µM and 0.5 µM of compound **8m** for 24 h. Cells were collected by trypsinisation, washed with 150 mM PBS and fixed with 70% ethanol for 30 min at 4 °C. After fixing, cells were again washed with PBS and stained with 400 µL of propidium iodide staining buffer [PI (200 µg), Triton X (100 µL), DNase-free RNase A (2 mg) in 10 mL of PBS] for 15 min in dark at room temperature. The samples were then analyzed for propidium iodide fluorescence from 15,000 events by flow cytometry using BD Accuri C6 flow-cytometer.

#### 4.2.5 *Hoechst staining*

SKOV-3 ovarian cancer cells were grown on coverslips in a 6 well plates ( $5 \times 10^5$  cells/well) and allowed to adhere for 24 h. The culture medium containing the compound **8m** at 0.1, 0.2 and 0.5 µM concentrations were added to cells. After 24 h incubation, culture medium was

removed; cells were washed with PBS and fixed with 4% formaldehyde solution at 4 °C for 10 min. Then cells were washed twice with PBS and stained with Hoechst 33242 (5 µg/mL) for 30 min at room temp. The excess dye was removed by washing twice with PBS and cell suspension were mounted on slides and were examined for morphological changes under fluorescence microscope using 350 nm excitation and 460 nm emission (Biorad, magnification 20x).

#### 4.2.6 Measurement of mitochondrial membrane potential ( $D\Psi_m$ )

SKOV-3 cells were cultured in 6 well plates at a density of  $5 \times 10^5$  cells/mL and allowed to adhere overnight. The cells were treated with 0.1, 0.2 and 0.5 µM of compound **8m** for 24 h. After 24 h treatment, the adherent cells were washed with PBS a solution of PBS containing JC-1 (5 µg/mL, Sigma) was added to each well and further incubated at room temperature for 30 minutes. Cells were washed two times with PBS to remove excess dye and were photographed in red and green channels using a fluorescence microscope at 20x magnification (Biorad).

#### 4.2.7 Reactive oxygen Species

SKOV-3 cells ( $2 \times 10^5$ /well) in a 6 well plate were incubated with the 0.1, 0.2 and 0.5 µM concentrations of the compound **8m** for 24 h. After incubation, cells were harvested with 0.05% trypsin-EDTA, washed with PBS and resuspended in 1 mL of PBS buffer containing 10 µM Carboxy-H<sub>2</sub>DCFDA (Thermofischer) at room temperature in the dark for 15 min. The excess dye was removed by washing with PBS, and the cells were immediately analyzed for green fluorescence using a BDC6-accuri flow cytometer.

#### 4.2.8 Caspase-3 assay

Caspase-3 activity in SKOV-3 cells was monitored using a colorimetric Caspase-3 Assay Kit (Thermo Fischer, khz0022). SKOV-3 cells ( $2 \times 10^5$  cells/well) were treated with 0.1, 0.2 and 0.5 µM concentrations of the compound **8m** for 24 h. Cells were harvested with 0.05% trypsin-EDTA and were lysed with lysis buffer (50 µL) for 20 min. Cell lysates were centrifuged at 15000 rpm for 10 min at 4 °C and the supernatant was added into 96-well plates. Final reaction buffer (50 µL) and caspase-3 substrate (Ac-DEVDpNA 5 µL) were then added to each well and the plates were incubated at 37 °C for 2 h. Optical density of the reactions in each well was measured at 405 nm with a plate reader (SpectraMax).

#### 4.2.9 Spheroid inhibition assay

SKOV-3 cells (5000 cells/well) were seeded in 96 well Ultra Low Attachment round-bottom plates and allowed to grow for 2 days to form spheroids. The spheroids were treated with 0.1, 0.2, 0.5  $\mu$ M concentrations of the gold complexes for a period of 72 h. The growth and surface area of the spheroids were monitored using phase contrast microscopy after 72 h treatment.

#### Acknowledgements

Authors are thankful to DoP, Ministry of Chemicals & Fertilizers, Govt. of India, New Delhi, for the award of NIPER fellowship. Dr. N. Shankaraiah thankful to SERB, DST, Govt. of India for the start-up grant (YSS-2015-001709).

#### 5.0 References

1. (a) M. Center, R. Siegel, A. Jemal, Global Cancer Facts and Figures, American Cancer Society, Atlanta, Georgia (2011) 1-52; (b) R.L. Siegel, K.D. Miller, A. Jemal, Cancer statistics, 2015. *CA Cancer J. Clin.* 65 (2015) 5-29.
2. X. Sui, R. Chen, Z. Wang, Z. Huang, N. Kong, M. Zhang, W. Han, F. Lou, J. Yang, Q. Zhang, X. Wang, C. He, H. Pan, Autophagy and chemotherapy resistance: a promising therapeutic target for cancer treatment, *Cell Death Dis.* 4 (2013) e838.
3. S. Elmore, Apoptosis: a review of programmed cell death, *Toxicologic Pathology.* 35 (2007) 495-516; (b) P. Sharma, T.S. Reddy, D. Thummuri, K.R. Senwar, N.P. Kumar, V.G.M. Naidu, S.K. Bhargava, N. Shankaraiah, Synthesis and biological evaluation of new benzimidazole-thiazolidinedione hybrids as potential cytotoxic and apoptosis inducing agents, *Eur. J. Med. Chem.* 124 (2016) 608-621; (c) S. Nekkanti, R. Tokala, N. Shankaraiah, Targeting DNA minor groove by hybrid molecules as anticancer agents, *Curr. Med. Chem.* 24 (2017) 2887-2907.
4. (a) A. Stoye, T.E. Peez, T. Opatz, Left, Right, or Both ? On the Configuration of the Phenanthroindolizidine alkaloid Tylophorine from *tylophora indica*, *J. Nat. Prod.* 76 (2013) 275-278; (b) L. Yang, L.H. Qin, S.A. Bligh, A. Bashall, C.F. Zhang, M. Zhang, Z.T. Wang, L.S. Xu, A new phenanthrene with a spiro lactone from *Dendrobium chrysanthum* and its anti-inflammatory activities, *Bioorg. Med. Chem.* 14 (2006) 3496-3501; (c) F.E. Koehn, G.T. Carter, The evolving role of natural products in drug

- discovery, *Nat. Rev. Drug Discovery*. 4 (2005) 206-220; (d) M. Sathish, B. Kavitha, V.L. Nayak, Y. Tangella, A. Ajitha, S. Nekkanti, A. Alarifi, N. Shankaraiah, N. Nagesh, A. Kamal, Synthesis of podophyllotoxin linked  $\beta$ -carboline congeners as potential anticancer agents and DNA topoisomerase II inhibitors, *Eur. J. Med. Chem.* 144 (2018) 557-571.
5. M. Deng, B. Su, H. Zhang, Y. Liu, Q. Wang, Total synthesis of phenanthroindolizidine alkaloids *via* asymmetric deprotonation of N-Boc-pyrrolidine, *RSC Adv.* 4 (2014) 14979-14984.
  6. (a) T. Ikeda, T. Yaegashi, T. Matsuzaki, R. Yamazaki, S. Hashimoto, S. Sawada, Synthesis of phenanthroindolizidine alkaloids and evaluation of their antitumor activities and toxicities, *Bioorg. Med. Chem. Lett.* 21 (2011) 5978-5981; (b) L. Wei, A. Brossi, R. Kendall, K.F. Bastow, S.L. Morris-Natschke, Q. Shi, K.H. Lee, Antitumor agents 251: Synthesis, cytotoxic evaluation, and structure-activity relationship studies of phenanthrene-based tylophorine derivatives (PBT's) as a new class of antitumor agents, *Bioorg. Med. Chem.* 14 (2006) 6560-6569.
  7. H.M. Faidallah, K.A. Shaikh, T.R. Sobahi, K.A. Khan, A.M. Asiri, An Efficient Approach to the Synthesis of Highly Congested 9,10-Dihydrophenanthrene-2,4-dicarbonitriles and Their Biological Evaluation as Antimicrobial Agents, *Molecules* 18 (2013) 15704-15716.
  8. (a) C.W. Yang, W.L. Chen, P.L. Wu, H.Y. Tseng, S.J. Lee, Anti-inflammatory mechanisms of phenanthroindolizidine alkaloids, *Mol. Pharmacol.* 69 (2006) 749-758.
  9. J.Y. Choi, W. Gao, J. Odegard, H.S. Shiah, M. Kashgarian, J.M. McNiff, D. C. Baker, Y.C. Cheng, J. Craft, Abrogation of skin disease in LUPUS-prone MRL/FAS<sup>ipr</sup> mice by means of a novel tylophorine analog, *Arthritis Rheum.* 54 (2006) 3277-3283.
  10. M.G. Banwell, A. Bezos, C. Burns, I. Kruszelnicki, C.R. Parish, S. Su, M.O. Sydnes, C8c-C15 monoseco-analogues of the phenanthroquinolizidine alkaloids julandine and cryptopleurine exhibiting potent anti-angiogenic properties, *Bioorg. Med. Chem. Lett.* 16 (2006) 181-185.
  11. X. Yang, Q. Shi, S-C. Yang, C-Y. Chen, S-L. Yu, K.F. Bastow, S.L.M. Natschke, P-C. Wu, C-Y. Lai, T-S. Wu, S-L. Pan, C-M. Teng, J-C. Lin, P-C. Yang, K-H. Lee, Antitumor Agents 288: Design, Synthesis, SAR, and Biological Studies of Novel Heteroatom-Incorporated Antofine and Cryptopleurine Analogues as Potent and Selective Antitumor Agents, *J. Med. Chem.* 54 (2011) 5097-5107; (b) S.R. Chemler, Phenanthroindolizidines and Phenanthroquinolizidines: Promising Alkaloids for Anti-Cancer Therapy, *Curr. Bioact Compd.* 5 (2009) 2-19; (c) D. Staerk, A.K. Lykkeberg, J. Christensen, B.A.

- Budnik, F. Abe, J.W. jaroszewski, *In vitro* cytotoxic activity of phenanthroindolizidine alkaloids from *Cynanchum vincetoxicum* and *Tylophora tanakae* against drug-sensitive and multidrug-resistant cancer cells, *J. Nat. Prod.* 65 (2002) 1299-1302.
12. K.N. Rao, R.K. Bhattacharya, S.R. Venkatachalam, Inhibition of thymidylate synthase and cell growth by the phenanthroindolizidine alkaloids pergularinine and tylophorinidine, *Chem-Biol. Interact.* 106 (1997) 201-212.
13. (a) W. Gao, A.P.-C. Chen, C.-H. Leung, E.A. Gullen, A. Furstner, Q. Shi, L. Wei, K.-H. Lee, Y.-C. Cheng, Structural analogs of tylophora alkaloids may not be functional analogs, *Bioorg. Med. Chem. Lett.* 18 (2008) 704-709; (b) X. Yang, Q. Shi, C.-Y. Lai, C.-Y. Chen, E. Ohkoshi, S.-C. Yang, C.-Y. Wang, K.F. Bastow, T.-S. Wu, S.-L. Pan, C.-M. Teng, P.-C. Yang, K.-H. Lee, Antitumor Agents 295. E-Ring Hydroxylated Antofine and Cryptopleurine Analogues as Antiproliferative Agents: Design, Synthesis, and Mechanistic Studies, *J. Med. Chem.* 55 (2012) 6751-6761.
14. W. Gao, W. Lam, S. Zhong, C. Kaczmarek, D.C. Baker, Y.C. Cheng, Novel mode of action of tylophorine analogs as antitumor compounds, *Cancer Res.* 64 (2004) 678-688.
15. Y. Wang, H.-C. Wong, E.A. Gullen, W. Lam, X. Yang, Q. Shi, K.H. Lee, Y.-C. Cheng, Cryptopleurine Analogs with Modification of E Ring Exhibit Different Mechanism to Rac-Cryptopleurine and Tylophorine, *Plos One* 7 (2012) e51138.
16. (a) Y. Fu, S.K. Lee, H.-Y. Min, T. Lee, J. Lee, M. Cheng, S. Kim, Synthesis and structure-activity studies of antofine analogues as potential anticancer agents, *Bioorg. Med. Chem. Lett.* 17 (2007) 97-100; (b) X. Yang, Q. Shi, K.F. Bastow, K.-H. Lee, Antitumor Agents. 274. A New Synthetic Strategy for E-Ring SAR Study of Antofine and Cryptopleurine Analogues, *Org. Lett.* 12 (2010) 1416-1419.
17. Y. Damayanthi, J.W. Lown, Podophyllotoxins: current status and recent developments, *Curr. Med. Chem.* 5 (1998) 205-252.
18. (a) H. Xu, M. Lv, X. Tian, A review on hemisynthesis, biosynthesis, biological activities, mode of action, and structure-activity relationship of podophyllotoxins: 2003-2007, *Curr. Med. Chem.* 16 (2009) 327-349; (b) B.A. Bhat, P.B. Reddy, S.K. Agrawal, A.K. Saxena, H.M.S. Kumar, G.N. Quazi, Studies on novel 4 $\beta$ -[(4-substituted)-1,2,3-triazol-1-yl] podophyllotoxins as potential anticancer agents, *Eur. J. Med. Chem.* 43 (2008) 2067-2072.
19. A. Kamal, J.R. Tamboli, M.V.P.S. Vishnuvardhan, S.F. Adil, V.L. Nayak, S. Ramakrishna, Synthesis and anticancer activity of heteroaromatic linked 4 $\beta$ -amido

- podophyllotoxins as apoptotic inducing agents, *Bioorg. Med. Chem. Lett.* 23 (2013) 273-280.
20. (a) Y. You, Podophyllotoxin Derivatives: Current Synthetic Approaches for New Anticancer Agents, *J. Curr. Pharm. Des.* 11 (2005) 1695-1717; (b) M. Gordaliza, M.A. Castro, J.M.M. Corall, A.S. Feliciano, Antitumor Properties of Podophyllotoxin and Related Compounds, *J. Curr. Pharm. Des.* 6 (2000) 1811-1839; (c) A. Kamal, T.S. Reddy, S. Polepalli, N. Shalini, V.G. Reddy, A.V.S. Rao, N. Jain, N. Shankaraiah, Synthesis and biological evaluation of podophyllotoxin congeners as tubulin polymerization inhibitors, *Bioorg. Med. Chem.* 22 (2014) 5466-5475.
21. W.J. Gensler, C.D. Murthy, M.H. Trammell, Nonenolizable podophyllotoxin derivatives, *J. Med. Chem.* 20 (1977) 635-644.
22. (a) Y. Hitotsuyanagi, M. Fukuyo, K. Tsuda, M. Kobayashi, A. Ozeki, H. Itokava, K. Takeya, 4-Aza-2,3-dehydro-4-deoxypodophyllotoxins: simple aza-podophyllotoxin analogues possessing potent cytotoxicity, *Bioorg. Med. Chem. Lett.* 10 (2000) 315-317; (b) I.V. Magedov, L. Frolova, M. Manpadi, U.D. Bhoga, H. Tang, N.M. Evdokimov, O. George, K.H. Georgiou, S. Renner, M. Getlik, T.L. Kinnibrugh, M.A. Fernandes, S.V. Slambrouck, W.F.A. steelant, C.B. Shuster, S. Rogelj, W.A. Otterlo, A. Kornienko, Anticancer Properties of an Important Drug Lead Podophyllotoxin Can Be Efficiently Mimicked by Diverse Heterocyclic Scaffolds Accessible via One-Step Synthesis, *J. Med. Chem.* 54 (2011) 4234-4246.
23. (a) P. Sharma, T.S. Reddy, N.P. Kumar, K.R. Senwar, S.K. Bhargava, N. Shankaraiah, Conventional and microwave-assisted synthesis of new 1*H*-benzimidazole-thiazolidinedione derivatives: A potential anticancer scaffold, *Eur. J. Med. Chem.* 138 (2017) 234-245; (b) M. Alvala, S. Bhatnagar, A. Ravi, V.U. Jeankumar, T.H. Manjashetty, P. Yogeeswari, D. Sriram, Novel acridinedione derivatives: Design, synthesis, SIRT1 enzyme and tumor cell growth inhibition studies, *Bioorg. Med. Chem. Lett.* 22 (2012) 3256-3260; (c) S. Nekkanti, K. Veeramani, N.P. Kumar, N. Shankaraiah, Microwave-assisted direct oxidative synthesis of  $\alpha$ -ketoamides from aryl methyl ketones and amines by a water soluble Cu (I)-complex, *Green Chem.* 18 (2016) 3439-3447.
24. (a) V.A. Chebanov, V.E. Saraev, S.M. Desenko, V.N. Chernenko, I.V. Knyazeva, U. Groth, T.N. Glasnov, C.O. Kappe, Tuning of Chemo- and Regioselectivities in Multi-component Condensations of 5-Aminopyrazoles, Dimedone, and Aldehydes, *J. Org. Chem.* 73 (2008) 5110-5118.

25. N. Ma, B. Jiang, G. Zhang, S-J. Tu, W. Wever, G. Li, New multi-component domino reactions (MDRs) in water: highly chemo-, regio- and stereoselective synthesis of spiro{[1,3]dioxanopyridine}-4,6-diones and pyrazolo[3,4-*b*]pyridines, *Green Chem.* 12 (2010) 1357-1361.
26. (a) M.G. Botes, S.C. Pelly, M.A.L. Blackie, A. Kornienko, W.A.L. van Otterlo, Synthesis of 4-azapodophyllotoxins with anticancer activity by multicomponent reactions, *Chem. Heterocycl. Compd.* 50 (2014) 119-138; (b) C-L. Shi, H. Chen, D-Q. Shi, An efficient one-pot synthesis of Pyrazolo[3,4-*b*]pyridinone derivatives catalyzed by L-proline, *J. Heterocyclic Chem.* 48 (2011) 351-354; (c) A.Y. Andriushchenko, S.M. Desenko, V.N. Chernenko, V.A. Chebanov, Green and Efficient Synthesis of Pyrazolo[3,4-*b*]quinolin-5-ones Derivatives by Microwave-Assisted Multi-component Reaction in Hot Water Medium, *J. Heterocycl. Chem.* 48 (2011) 365-367; (d) F. Shi, X.-N. Zeng, G. Zhang, N. Ma, B. Jiang, S. Tu, *Bioorg. Med. Chem. Lett.* 21 (2011) 7119-7123.
27. N. Jeedimalla, M. Flint, L. Smith, A. Haces, D. Minond, S.P. Roche, Multi-component assembly of 4-aza-podophyllotoxins: A fast entry to highly selective and potent anti-leukemic agents, *Eur. J. Med. Chem.* 106 (2015) 167-179.
28. S. Kandil, J.M. Wyamant, B.M. Kariuki, A.T. Jones, C. McGuigan, A.D. Westwell, Novel cis-selective and non-epimerisable C3-hydroxy azapodophyllotoxins targeting microtubules in cancer cells, *Eur. J. Med. Chem.* 110 (2016) 311-325.
29. (a) K. Wang, Y. Hu, M. Wu, Z. Li, Z. Liu, B. Su, A. Yu, Y. Liu, Q. Wang, *m*-CPBA/TFA: an efficient nonmetallic reagent for oxidative coupling of 1,2-diarylethylenes, *Tetrahedron* 66 (2010) 9135-9140; (b) Y.Z. Lee, C.W. Yang, H.Y. Hsu, Y.Q. Qiu, T.K. Yeh, H.Y. Chang, Y.S. Chao, S.J. Lee, Synthesis and Biological Evaluation of Tylophorine-Derived Dibenzoquinolines as Orally Active Agents: Exploration of the Role of Tylophorine E Ring on Biological Activity, *J. Med. Chem.* 55 (2012) 10363-10377; (c) N.P. Kumar, P. Sharma, T.S. Reddy, S. Nekkanti, N. Shankaraiah, G. Lalita, S. Sujanakumari, S.K. Bhargava, V.G.M. Naidu, A. Kamal, Synthesis of 2,3,6,7-tetramethoxyphenanthrene-9-amine: An efficient precursor to access new 4-aza-2,3-dihydropyridophenanthrenes as apoptosis inducing agents, *Eur. J. Med. Chem.* 127 (2017) 305-317 (d) T.R. Govindachari, M. Lakshmikantham, K. Nagarajan, B. Pai, Chemical examination of *Tylophora asthmatica*-II, *Tetrahedron* 4 (1958) 311-324.
30. (a) T. Mosmann, Rapid colorimetric assay for cellular growth and survival: application to proliferation and cytotoxicity assays, *J. Immunol. Meth.* 65 (1983) 55-63; (b) P. Sharma, K.R. Senwar, M.K. Jeengar, T.S. Reddy, V.G.M. Naidu, A. Kamal, N. Shankaraiah,

- H<sub>2</sub>O-mediated isatin spiro-epoxide ring opening with NaCN: Synthesis of novel 3-tetrazolylmethyl-3-hydroxy-oxindole hybrids and their anticancer evaluation, *Eur. J. Med. Chem.* 104 (2015) 11-24.
31. (a) C.L. Clainche, M. F. Carlier, Regulation of actin assembly associated with protrusion and adhesion in cell migration, *Physiol. Rev.* 88 (2008) 489-513; (b) G. Lorente, E. Syriani, M. Morales, Actin Filaments at the Leading Edge of Cancer Cells are Characterized by a High Mobile Fraction and Turnover Regulation by Profilin, *PloS one* 9 (2014) e85817; (c) D. Vignjevic, G. Montagnac, Reorganisation of the dendritic actin network during cancer cell migration and invasion, *Semin. Cancer Biol.* 18 (2008) 12-22; (d) M.P. Sheetz, D. Felsenfeld, C. Galbraith, D. Choquet, Cell migration as a five-step cycle, *Biochem. Soc. Symp.* 65 (1999) 233–243.
32. K.R. Senwar, T.S. Reddy, D. Thummuri, P. Sharma, V.G.M. Naidu, G. Srinivasulu, N. Shankaraiah, Design, synthesis and apoptosis inducing effect of novel (Z)-3-(3'-methoxy-4'-(2-amino-2-oxoethoxy)-benzylidene)indolin-2-ones as potential antitumour agents, *Eur. J. Med. Chem.* 118 (2016) 34-36.
33. (a) P. Pozarowski, Z. Darzynkiewicz, Analysis of cell cycle by flow cytometry, *Methods. Mol. Biol.* 281 (2004) 301-311; (b) Y.R. Wang, Y. Xu, Z.Z. Jiang, M. Guerram, B. Wang, X. Zhu, L.Y. Zhang, Deoxypodophyllotoxin Induces G2/M Cell Cycle Arrest and Apoptosis in SGC-7901 Cells and Inhibits Tumor Growth *in Vivo*, *Molecules.* 20 (2015) 1661-1675; (c) S.Y. Shin, Y. Yong, C.G. Kim, Y.H. Lee, Y. Lim, Deoxypodophyllotoxin induces G2/M cell cycle arrest and apoptosis in HeLa cells, *Cancer Lett.* 287 (2010) 231-239.
34. (a) S. Reid, R. Cross, E.C. Snow, Combined Hoechst 33342 and merocyanine 540 staining to examine murine B cell cycle stage, viability and apoptosis, *J. Immunol. Methods.* 192 (1996) 43-54; (b) J. Yan, Y. Pang, J. Chen, J. Sheng, J. Hu, L. Huang, X. Li, Synthesis, biological evaluation and mechanism study of a class of cyclic combretastatin A-4 analogues as novel antitumour agents, *RSC Adv.* 5 (2015) 98527-98537; (c) T. Frey, Nucleic acid dyes for detection of apoptosis in live cells, *Cytometry* 21 (1995) 265-274.
35. X-C. Huang, L. Jin, M. Wang, D. Liang, Z-F. Chen, Y. Zhang, Y-M. Pan, H.S.Wang, Design, synthesis and *in vitro* evaluation of novel dehydroabietic acid derivatives containing a dipeptide moiety as potential anticancer agents, *Eur. J. Med. Chem.* 89 (2015) 370-385.

36. T.S. Reddy, V.G. Reddy, H. Kulhari, R. Shukla, A. Kamal, V. Bansal, Synthesis of (Z)-1-(1,3-diphenyl-1H-pyrazol-4-yl)-3-(phenylamino)prop-2-en-1-one derivatives as potential anticancer and apoptosis inducing agents, *Eur. J. Med. Chem.* 117 (2016) 157-166.
37. (a) V. Gurtu, S.R. Kain, G. Zhang, Fluorometric and colorimetric detection of caspase activity associated with apoptosis, *Anal. Bio Chem.* 251 (1997) 98-102; (b) Y. Pan, M. Guo, Z. Nie, Y. Huang, Y. Peng, A. Liu, M. Qing, S. Yao, Colorimetric detection of apoptosis based on caspase-3 activity assay using unmodified gold nanoparticles, *Chem. Commun.* 48 (2012) 997-999.
38. (a) H-Y. Lee, A-C. Tsai, M-C. Chen, P-J. Shen, Y.C. Cheng, C-C. Kuo, S-L. Pan, Y-M. Liu, J-F. Liu, T-K. Yeh, J-C. Wang, C-Y. Chang, J-Y. Chang, J-P. Liou, Azaindolylsulfonamides, with a More Selective Inhibitory Effect on Histone Deacetylase 6 Activity, Exhibit Antitumor Activity in Colorectal Cancer HCT116 Cells, *J. Med. Chem.* 57 (2014) 4009-4022; (b) M. Asif, M.A. Iqbal, M.A. Hussein, C.E. Oon, R.A. Haque, M.B.K. Ahamed, A.S.A. Majid, A.M.S.A. Majid, Human colon cancer targeted pro-apoptotic, anti-metastatic and cytostatic effects of binuclear Silver(I)-N-Heterocyclic carbene (NHC) complexes, *Eur. J. Med. Chem.* 108 (2016) 177-187.

### Tables/Figures/Scheme captions

**Table 1.** Optimization of the reaction conditions to phenanthrene fused-tetrahydrodibenzoacridinone **8a**

**Table 2.** *In vitro* cytotoxic activity ( $IC_{50}$  in  $\mu M$ )<sup>a</sup> of phenanthrene fused-dihydrodibenzoquinolin-ones **8a-r**

**Figure 1.** Structures of phenanthrene alkaloids, azapodophyllotoxin derivatives and newly designed molecules.

**Figure 2.** Structure activity relationship (SAR) of phenanthrene fused-tetrahydrodibenzoacridinone derivatives.

**Figure 3.** Effect of compound **8m** on F-actin in SKOV-3 cells. The cells were treated with 0.1, 0.2 and 0.5  $\mu M$  concentrations of **8m**. Compound **8m** induced disruption of stress fibre network. F-actin was stained with rhodamine phalloidin (red fluorescent dye). The blue colour indicates Hoechst 33242 staining for nucleus.

**Figure 4.** SKOV-3 ovarian cancer cells were treated with compound **8m** for 24 h. (A) The cell cycle distribution was analysed by using propidium iodide staining method and analysed by flow cytometry (BDc6 accuri). (B) Data of 10,000 cells were collected for each data file. The percentage of cell population in G0/G1, S and G2/M phase were calculated by using BDc6accuri software

**Figure 5.** Compound **8m** induced morphological changes in SKOV-3 cells observed by Hoechst staining.

**Figure 6.** JC-1 mitochondrial staining of SKOV-3 cells after treatment with 0.1, 0.2 and 0.5  $\mu\text{M}$  concentrations of **8m**. DMSO treated cells were used as control.

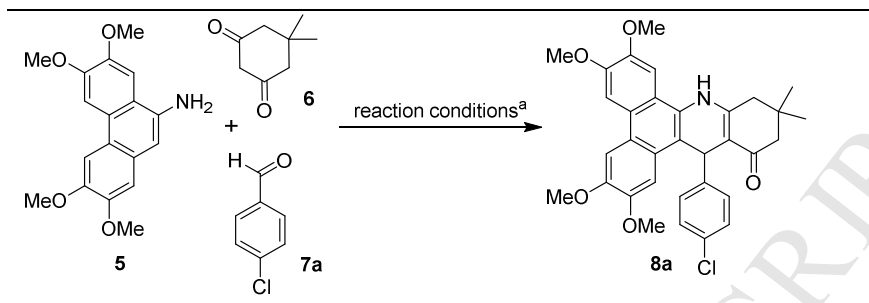
**Figure 7.** Effect of **8m** on reactive oxygen species. SKOV-3 cells were treated with 0.1, 0.2 and 0.5  $\mu\text{M}$  of **8m**, and incubated with Carboxy- $\text{H}_2\text{DCFDA}$ . The DCF fluorescence was quantified by using flowcytometer.

**Figure 8.** Effect of compound **8m** on Caspase-3 activity; SKOV-3 cells were treated with compound **8m** and the activity of caspase-3 was determined using caspase-3 colorimetric assay kit.

**Figure 9.** Compound **8m** caused greater inhibition of tumor spheroid growth. An ultra low attachment (ULA) 96-well round-bottomed plate was used to generate SKOV-3 tumor spheroids.

**Scheme 1.** Microwave-assisted one-pot synthesis of various phenanthrene fused-tetrahydrodibenzo-acridinones **8a-r**.

## Tables/Figures/Schemes

**Table 1.** Optimization of the reaction conditions to phenanthrene fused-tetrahydrobenzoacridinone **8a**


The reaction scheme shows the synthesis of compound **8a** from starting materials **5**, **6**, and **7a**. Compound **5** is a phenanthrene derivative with methoxy groups at positions 1, 3, 4, and 8, and an amino group at position 9. Compound **6** is a cyclic amide with a quaternary carbon. Compound **7a** is 4-chlorobenzaldehyde. The reaction conditions are indicated as 'reaction conditions<sup>a</sup>'.

entry	method	solvent	temperature (°C)	time (min)	yield (%) <sup>b</sup>
1.	conventional	EtOH	80	180	61
2.	conventional	EtOH	80	300	65
3.	MW	EtOH	100	30	69
4.	MW	EtOH	120	10	77
5.	MW	EtOH	120	30	80
6.	<b>MW</b>	<b>EtOH</b>	<b>150</b>	<b>20</b>	<b>91</b>
7.	MW	EtOH	150	30	91
8.	MW	H <sub>2</sub> O	100	12	-

<sup>a</sup>Reaction conditions: **5** (0.28 mmol), **6** (0.28 mmol), **7** (0.28 mmol) and solvent (3 mL) .

<sup>b</sup>Isolated yields. MW: microwave heating conditions.

**Table 2.** *In vitro* cytotoxic activity (IC<sub>50</sub> in  $\mu\text{M}$ )<sup>a</sup> of phenanthrene fused-dihydrodibenzo-quinolin-ones **8a–r**

Compound	HeLa <sup>b</sup>	PC-3 <sup>c</sup>	HT-1080 <sup>d</sup>	SKOV-3 <sup>e</sup>	Hek-293T <sup>f</sup>
<b>8a</b>	38.8±2.51	>50	30.1±1.34	15.89±1.0	>50
<b>8b</b>	28.1±3.62	17.6±2.33	21.3±1.16	13.7±1.81	43.5±1.78
<b>8c</b>	>50	31.4±1.64	15.6±0.89	18.6±1.64	35.7±2.98
<b>8d</b>	>50	>50	32.3±2.26	11.5±0.26	25.7±1.34
<b>8e</b>	12.1±2.15	8.90±0.57	16.3±0.85	10.8±0.43	29.2±1.78
<b>8f</b>	31.6±1.82	12.4±0.88	11.6±0.34	15.5±1.94	36.3±2.54
<b>8g</b>	11.7±0.89	23.8±1.85	9.83±0.61	13.6±0.18	>50
<b>8h</b>	9.42±0.65	6.84±0.12	7.64±0.55	6.5±0.37	>50
<b>8i</b>	1.35±0.24	7.70±0.35	4.32±0.15	4.66±0.22	24.6±1.37
<b>8j</b>	>50	>50	25.7±1.43	11.5±1.23	>50
<b>8k</b>	4.79±0.71	7.17±0.87	5.63±0.19	1.62±0.24	38.9±1.68
<b>8l</b>	2.62±0.33	5.79±0.38	2.62±0.11	0.61±0.08	28.3±1.32
<b>8m</b>	4.38±0.95	11.8±0.47	3.89±0.27	0.24±0.05	18.5±0.89
<b>8n</b>	13.6±1.54	5.67±0.73	11.65±0.37	4.81±0.35	41.5±0.51
<b>8o</b>	2.28±0.52	7.10±0.57	5.87±0.17	1.6±0.31	18.9±1.32
<b>8p</b>	3.7±0.87	21.6±0.93	8.85±0.29	2.89±0.24	33.5±1.66
<b>8q</b>	2.46±0.36	5.89±0.19	3.78±0.26	2.35±1.23	15.5±0.78
<b>8r</b>	6.87±0.81	5.31±0.23	3.83±0.08	2.67±0.09	14.37±1.2
<b>Cisplatin<sup>g</sup></b>	3.35±0.16	6.34±0.21	0.89±0.06	1.89±0.32	4.78±0.35

<sup>a</sup>50% Inhibitory concentration after 48 h of compound treatment; <sup>b</sup>cervical cancer cells; <sup>c</sup>prostate cancer cells; <sup>d</sup>fibrosarcoma cancer cells; <sup>e</sup>ovarian cancer cells; <sup>f</sup>normal kidney cells; <sup>g</sup>Cisplatin as a positive control.

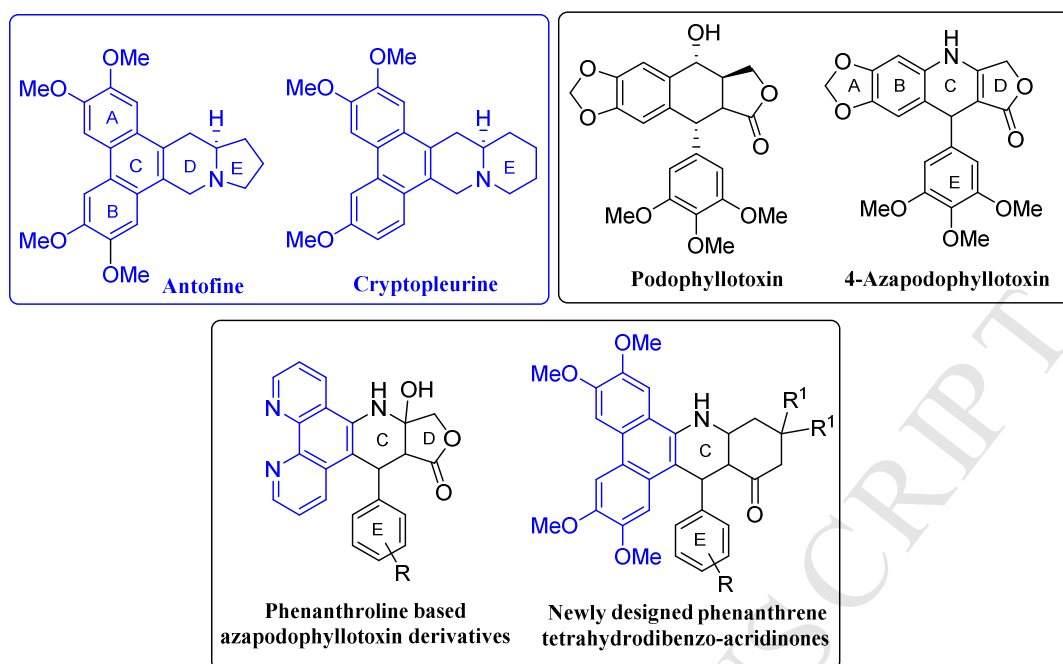


**Figure 1.** Structures of phenanthrene alkaloids, azapodophyllotoxin derivatives and newly designed molecules.

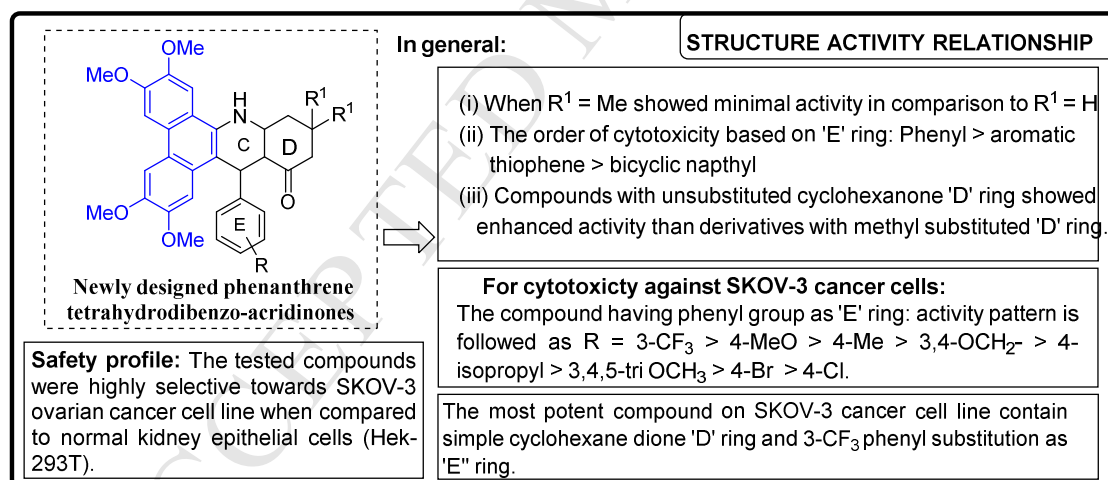


**Figure 2.** Structure activity relationship (SAR) of phenanthrene fused-tetrahydrodibenzo-acridinone derivatives.

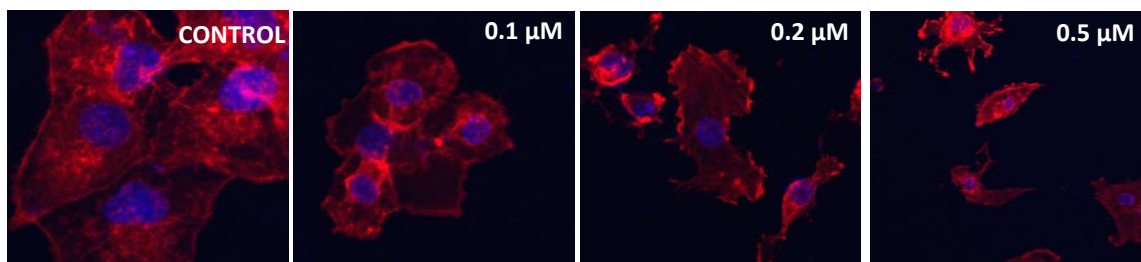


**Figure 3.** Effect of compound **8m** on F-actin in SKOV-3 cells. The cells were treated with 0.1, 0.2 and 0.5  $\mu\text{M}$  concentrations of **8m**. Compound **8m** induced disruption of stress fibre network. F-actin was stained with rhodamine phalloidin (red fluorescent dye). The blue colour indicates Hoechst 33242 staining for nucleus.

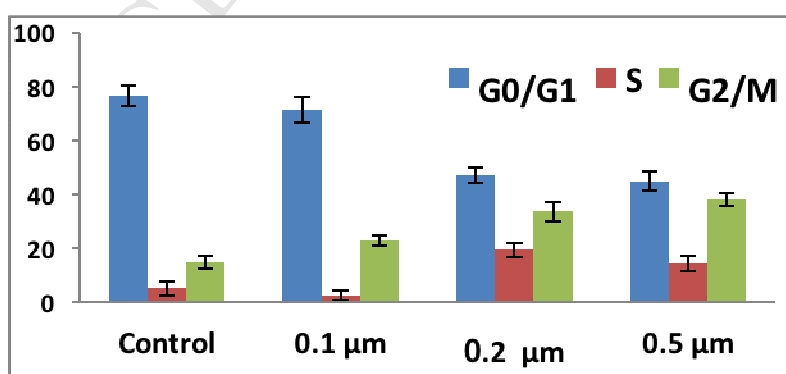
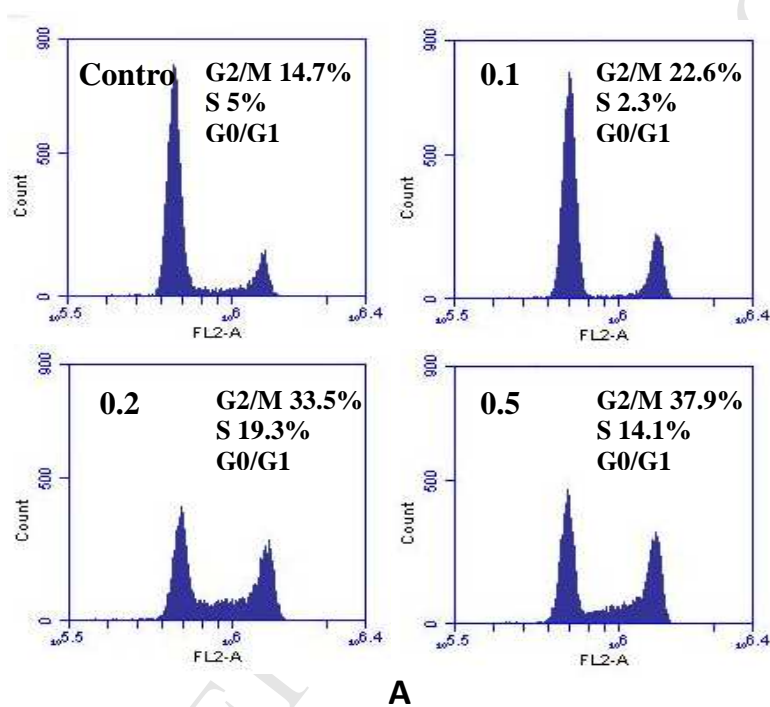


**Figure 4.** SKOV-3 ovarian cancer cells were treated with compound **8m** for 24 h. (A) The cell cycle distribution was analysed by using propidium iodide staining method and analysed

by flow cytometry (BDc6 accuri). **(B)** Data of 10,000 cells were collected for each data file. The percentage of cell population in G0/G1, S and G2/M phase were calculated by using BDc6accuri software.

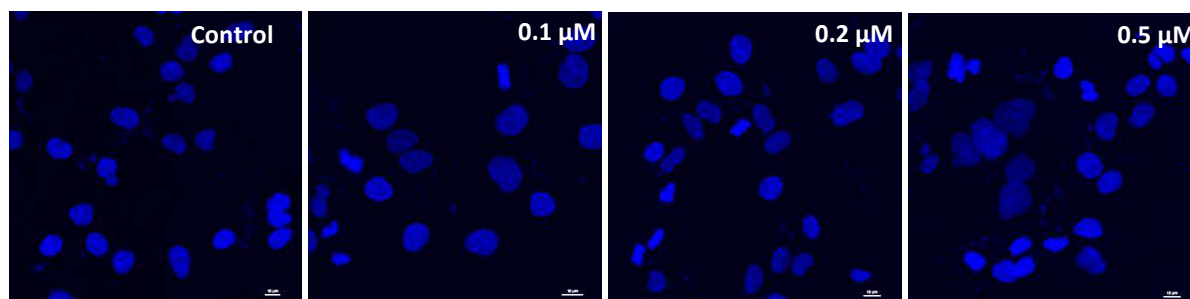


**Figure 5.** Compound **8m** induced morphological changes in SKOV-3 cells observed by Hoechst staining.

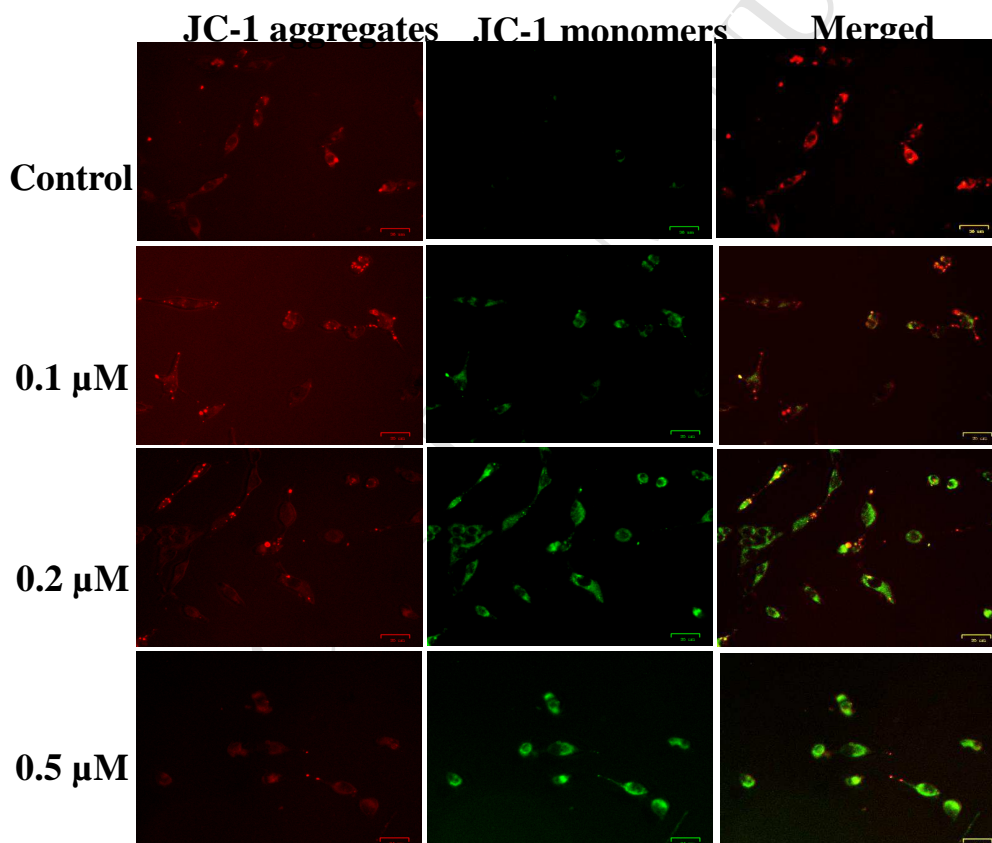


**Figure 6.** JC-1 mitochondrial staining of SKOV-3 cells after treatment with 0.1, 0.2 and 0.5 μM concentrations of **8m**. DMSO treated cells were used as control.

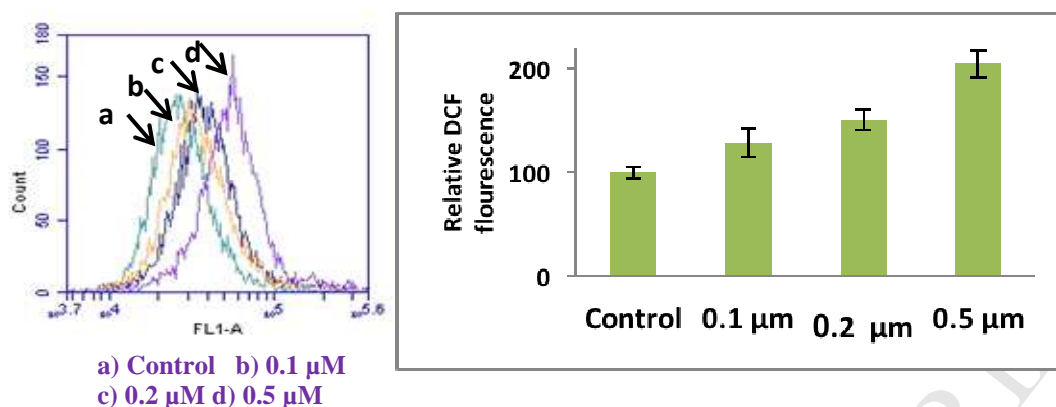


**Figure 7.** Effect of **8m** on reactive oxygen species. SKOV-3 cells were treated with 0.1, 0.2 and 0.5 μM of **8m**, and incubated with Carboxy-H<sub>2</sub>DCFDA. The DCF fluorescence was quantified by using flowcytometer.

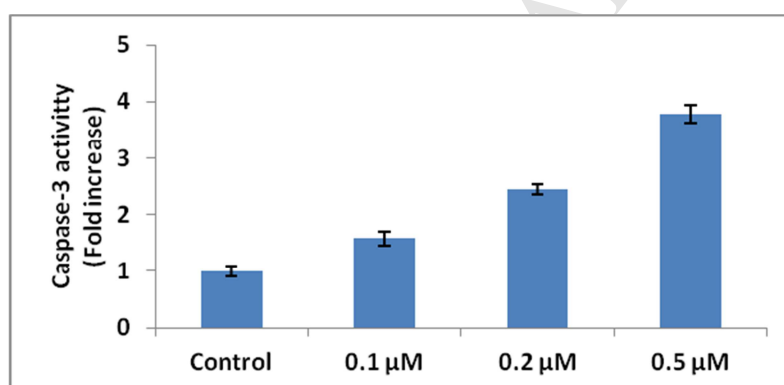


**Figure 8.** Effect of compound **8m** on Caspase-3 activity; SKOV-3 cells were treated with compound **8m** and the activity of caspase-3 was determined using caspase-3 colorimetric assay kit.

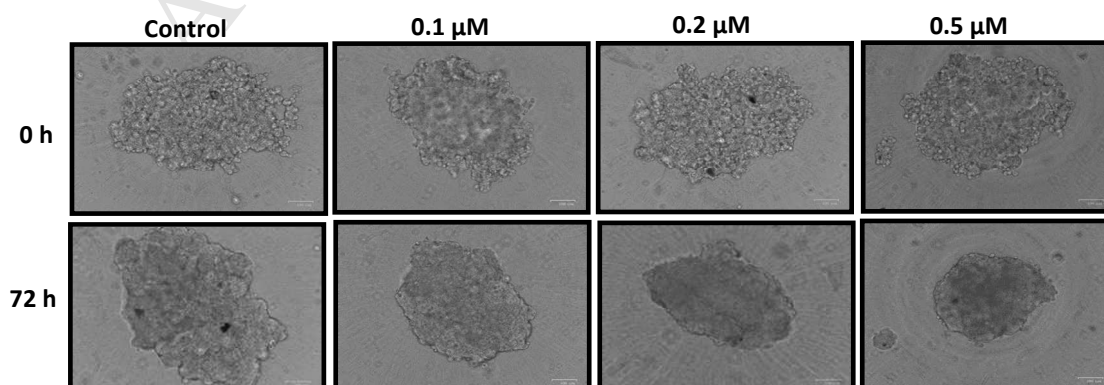
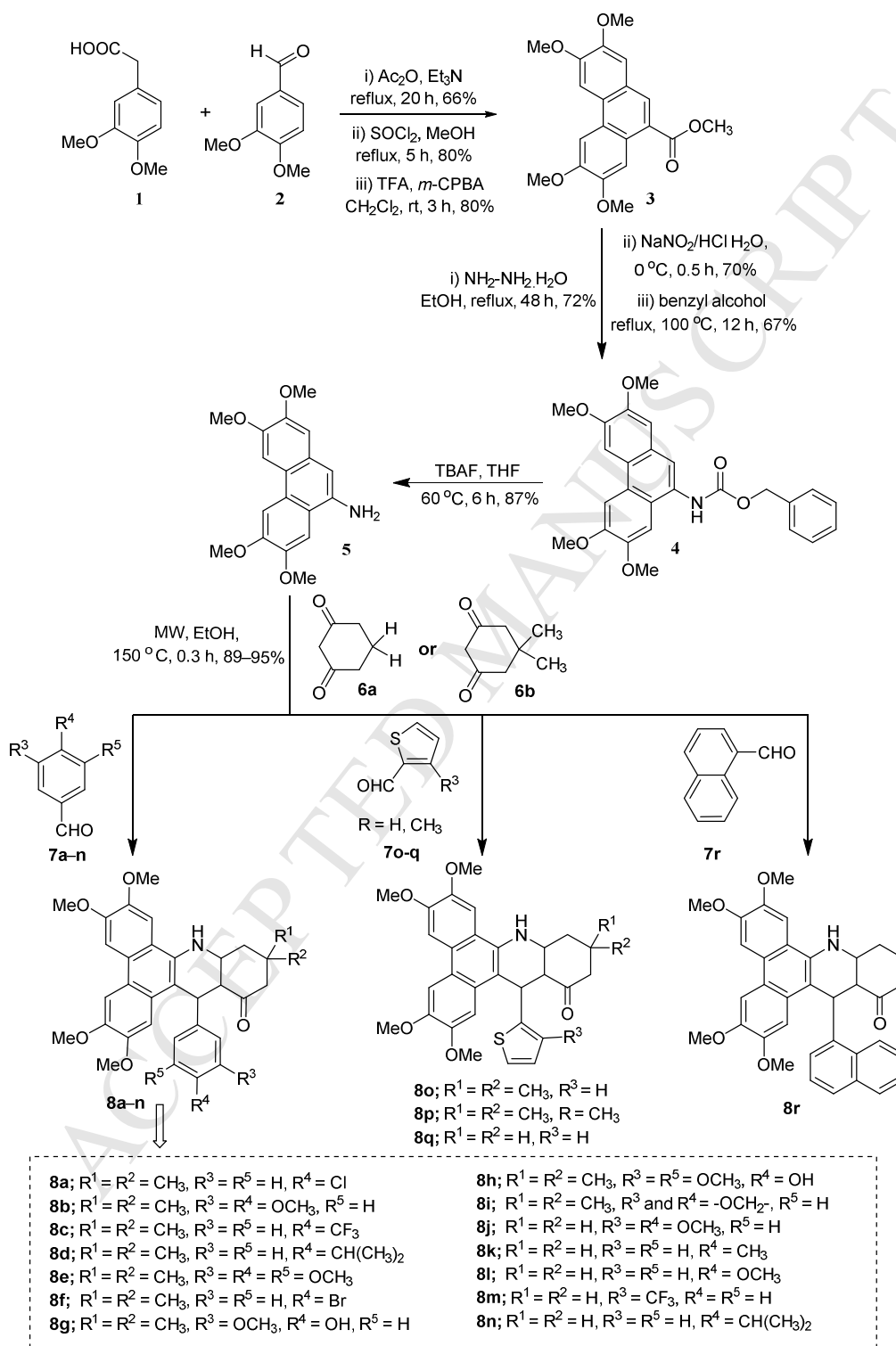


**Figure 9.** Compound **8m** caused greater inhibition of tumor spheroid growth. An ultra low attachment (ULA) 96-well round-bottomed plate was used to generate SKOV-3 tumor spheroids.



**Scheme 1.** Microwave-assisted one-pot synthesis of various phenanthrene fused-tetrahydrodibenzo-acridinones **8a–r**

**Research Highlights**

- Fast access to phenanthrene fused-tetrahydrodibenzo-acridinones by one-pot synthesis.
- Cytotoxicity on selected cancer cell lines and apoptosis inducing studies.
- In SKOV-3 ovarian cancer cells, **8m** inhibited F-actin and spheroidal growth.
- Compound **8m** induced dose dependent G2/M cell cycle arrest in SKOV-3 cells.
- **8m** caused the collapse of mitochondrial potential and activated caspase-3.